Marine Environmental Research 199 (2024) 106621

Contents lists available at ScienceDirect

Marine Environmental Research

journal homepage: www.elsevier.com/locate/marenvrev

Variability in zoobenthic blue carbon storage across a southern polar gradient

Bétina A.V. Frinault [a,*], David K.A. Barnes [b]

[a] School of Geography and the Environment, Oxford University Centre for the Environment, University of Oxford, South Parks Road, Oxford, OX1 3QY, UK
[b] British Antarctic Survey, UK Research and Innovation, Madingley Road, Cambridge, CB3 0ET, UK

ARTICLE INFO

Keywords:
Zoobenthic carbon storage
Blue carbon
Antarctic
Benthos
Climate change
Ecosystem function
Functional groups
Vulnerable marine ecosystems
Dropstones
Ecosystem service
Ice-cover loss

ABSTRACT

The seabed of the Antarctic continental shelf hosts most of Antarctica's known species, including taxa considered indicative of vulnerable marine ecosystems (VMEs). Nonetheless, the potential impact of climatic and environmental change, including marine icescape transition, on Antarctic shelf zoobenthos, and their blue carbon-associated function, is still poorly characterised. To help narrow knowledge gaps, four continental shelf study areas, spanning a southern polar gradient, were investigated for zoobenthic (principally epi-faunal) carbon storage (a component of blue carbon), and potential environmental influences, employing a functional group approach. Zoobenthic carbon storage was highest at the two southernmost study areas (with a mean estimate of 41.6 versus 7.2 g C m^{-2}) and, at each study area, increased with morphotaxa richness, overall faunal density, and VME indicator density. Functional group mean carbon content varied with study area, as did each group's percentage contribution to carbon storage and faunal density. Of the environmental variables explored, sea-ice cover and primary production, both likely to be strongly impacted by climate change, featured in variable subsets most highly correlating with assemblage and carbon storage (by functional groups) structures. The study findings can underpin biodiversity- and climate-considerate marine spatial planning and conservation measures in the Southern Ocean.

1. Introduction

This century sees the tercentenary of the Industrial Revolution, and over the corresponding period, atmospheric levels of greenhouse gases (GHGs) have been rising. The atmospheric concentration of the most ubiquitous GHG, carbon dioxide (CO_2), has increased from around 280 parts per million (ppm) in 1750, i.e., pre-industrial-era, to a 2022 average of ~417 ppm; this rise being particularly significant in the last 75 years and mainly from intensities of fossil-fuel combustion, cement production, and deforestation, i.e., anthropogenic (Friedlingstein et al., 2023; IPCC, 2023). The cumulative effect of GHG emissions is global climate change, including warming, the impacts of which are increasingly experienced across the world and considered intertwined with the biodiversity crisis (IPCC, 2022, 2023; Pörtner et al., 2023; Siegert et al., 2023). To reduce levels of atmospheric CO_2, societal efforts centre on minimising emissions at source (i.e., decarbonisation methodologies) and large-scale CO_2 capture; the captured CO_2 later used in further processes or potentially placed in long-term geological storage, e.g., within depleted oil and gas reservoirs of continental shelves – legacies of hydrocarbon extraction (Holloway and Burnard, 2009; Luo et al., 2023). In parallel, protection and capacity enhancement of natural carbon sinks, including, for example, the living resources/biomass of various marine ecosystems such as those present along tropical and temperate shorelines (e.g., McLeod et al., 2011; Greiner et al., 2013; Howard et al., 2014; Song et al., 2023) and on high-latitude/polar continental shelves (e.g., Gogarty et al., 2020; Cavanagh et al., 2021; Bax et al., 2022), are also being pursued.

The vast ocean network, constituting >70% of the world's surface, plays a major role in mitigating climate change by helping regulate atmospheric levels of CO_2, the oceans collectively absorbing ~26% of anthropogenic CO_2 emissions (Friedlingstein et al., 2023) and the Southern Ocean, representing ~10% of the ocean network, disproportionately accounting for around one-quarter of total oceanic uptake of atmospheric CO_2 (Arrigo et al., 2008). Marine biodiversity can help support this process through "blue carbon", a component of which can be defined as the carbon captured and stored by marine life, i.e., the carbon within living marine biomass (Barnes, 2018). Blue carbon is also considered a marine ecosystem service benefitting humankind (Grant

* Corresponding author.
E-mail address: betina.frinault@ouce.ox.ac.uk (B.A.V. Frinault).

https://doi.org/10.1016/j.marenvres.2024.106621
Received 18 March 2024; Received in revised form 19 June 2024; Accepted 20 June 2024
Available online 22 June 2024

et al., 2013; Rogers et al., 2020; Cavanagh et al., 2021). Marine primary producers, such as phytoplankton and macroalgae, initially capture CO_2 via photosynthesis, and thereafter, carbon is exported/transferred within associated and conjugated ecosystems (Cavan and Hill, 2022), being stored across the marine food web over diverse timespans and spatial scales, eventually leading to its sequestration within seabed sediments (Barnes, 2018).

In the polar regions, biological carbon pathways (and fates) are yet to be fully understood (Cartapanis et al., 2016; Henley et al., 2020; Sands et al., 2023); however, at high-temperate, sub-polar and polar latitudes, marine food webs can be based on macroalgae (e.g., kelp; see Vilas et al., 2020) and phytoplankton (microalgae), and at the very highest latitudes of the Southern Ocean and its constituent seas, phytoplankton dominate primary production (Deppeler and Davidson, 2017). In the cold surface waters of the Antarctic, where atmospheric CO_2 more readily dissolves (Arrigo et al., 2008), huge seasonal (austral spring and summer) accumulations (blooms) of phytoplankton capture CO_2, incorporating it into the biological carbon cycle and initiating pathways for carbon storage in the Antarctic marine food web, including in the zoobenthos (seafloor-dwelling animals), by which an estimated 12–18% of Southern Ocean primary production is consumed (Barnes, 2017, Fi g. 8 in Henley et al., 2020). The seafloor is also where the majority of Antarctica's known biodiversity resides (De Broyer et al., 2014) and where taxa considered indicative of vulnerable marine ecosystems (VMEs), as defined by the Commission for the Conservation of Antarctic Marine Living Resources (CCAMLR; CCAMLR, 2009), have been observed (CCAMLR, 2019; Lockhart and Hocevar, 2021). The presence of VME indicator taxa can strengthen justification for the adoption of proposed regional protection frameworks, such as Marine Protected Areas (MPAs) (Lockhart and Hocevar, 2021), and some VME indicators, e.g., corals, owing to their carbonate skeletons, are particularly proficient at storing carbon (and enhancing sequestration, i.e., long-term storage potential) (Barnes, 2018) whilst some are also important habitat providers/ecosystem engineers (Miller et al., 2012); hence, can help amplify carbon storage through associated inhabitants.

Similar to terrestrial forests and coastal wetlands (Howard et al., 2014; Mildrexler et al., 2020), marine biodiversity can be important in capturing, storing and facilitating sequestration of carbon. Carbon that might otherwise be broken down and recycled by the microbial loop is taken up and bound into tissues (and skeletons) of marine biota (Barnes, 2018). Benthic habitats, including, for example, their biological/zoobenthic communities (and component assemblages), i.e., the fauna living on (epi-faunal) and within (in-faunal) the seabed, can function as carbon sinks, accumulating and immobilising carbon (see Peck et al., 2010; Alurralde et al., 2019; Barnes et al., 2020). Zoobenthic assemblages, in terms of their composition, are known to be shaped by various combinations of environmental variables, such as ice cover, substratum type and physical/chemical features of the seabed (e.g., Domack et al., 2005; Isla et al., 2006; Niemann et al., 2009; Clark et al., 2017; Post et al., 2017; Ziegler et al., 2017; Almond et al., 2021). Alterations in such variables may impact the structure and function (including performance) of assemblages. Disentangling bio-physical relationships can be helpful for predictions regarding biological responses to environmental change (Cummings et al., 2018). To discern benthic community/assemblage structure epi-zoobenthos (the epifaunal component of zoobenthos) can be sampled/surveyed by relatively non-destructive means, e.g., via seafloor imaging techniques, whereas in-fauna are generally sampled by (more intrusive) sediment cores and grabs (Pineda-Metz and Gerdes, 2018). Although in-faunal organisms do not fall within the remit of the current study, they can account for ~50% of the carbon stored in the benthos (when epifauna and infauna are both considered), for example, of Antarctic fjords (Zwerschke et al., 2022).

Studies assessing high-latitude benthic blue carbon, including within the context of ecosystem services and nature-based solutions to moderating climate change, are growing yet still relatively rare. Furthermore, such studies are primarily conducted within exclusive economic zones or performed in consideration of unilateral marine protection zones (e.g., Barnes et al., 2019, 2021a; Bax et al., 2022); this opposed to, for example, internationally-shared waters or areas beyond national jurisdiction. If left undisturbed, these seabed ecosystems may continue functioning as carbon sinks and store carbon delivered to them through the food web (Sands et al., 2023). However, given ongoing and anticipated environmental shifts in high-latitude marine environments brought about by climate change and direct human impacts associated with the Anthropocene (Steffen et al., 2011), Antarctic seafloor habitats, their component communities/assemblages, and their associated functions and services may alter in response or indeed be at risk (Rogers et al., 2020; Cavanagh et al., 2021; Gutt et al., 2021).

Over the past few decades, carbon storage in polar zoobenthic communities has garnered attention in both hemispheres. Several investigations have now employed blue-carbon-oriented "functional groups" – a faunal grouping method in which fauna are grouped based on functional traits considered important in benthic blue carbon pathways (see Barnes and Sands, 2017). For example, studies in the Barents Sea, where carbon storage capacities, also referred to as "carbon standing stocks", of sedimented continental shelf assemblages were assessed (Souster et al., 2020, 2024), and in deglaciating fjords of the western Antarctic Peninsula, where blue carbon of emerging coastal benthic ecosystems was evaluated (Barnes et al., 2020; Zwerschke et al., 2022). Emergent polar marine habitats experiencing losses of overlying ice (e.g., sea ice, glaciers and ice shelves) are, in particular, regarded as potentially large-scale negative feedbacks on climate change (Peck et al., 2010; Morley et al., 2022; Zwerschke et al., 2022; Sands et al., 2023).

Antarctic seabed biodiversity, having developed in relative constancy of physical conditions and partial isolation due to the presence of the Antarctic Circumpolar Current (ACC) (Arntz et al., 1994), is likely vulnerable to climate change and associated environmental alterations (Rogers et al., 2020; Gutt et al., 2021; Casado et al., 2023). Nevertheless, considerable knowledge gaps exist around how high-latitude zoobenthic communities, and their carbon storage function, may alter in a warming world and as marine icescapes modify (however, see Barnes, 2017; Pineda-Metz et al., 2020). In respect, this study aims to discern how zoobenthic carbon storage varies across a southern polar gradient and examines zoobenthic (principally epi-zoobenthic) assemblages of four continental/island shelf study areas, all connected by the Scotia Arc, and representative of a transition from cool to seasonally-surface-freezing marine waters. The study includes the following objectives: (i) to ascertain whether zoobenthic carbon storage variance aligns with biodiversity measures (richness) and faunal density; (ii) to determine if VME indicator taxa substantially contribute to zoobenthic carbon storage; (iii) to explore functional groups' contributions to zoobenthic carbon storage; and, finally, (iv) to identify potential environmental drivers of zoobenthic carbon storage, including whether dropstones, physical features of the seabed, exhibit a discernible influence. The wider aims of this study include furthering the knowledge base of very high-latitude blue carbon estates in a warming world with anticipated marine icescape transformation, and providing an indication of the zoobenthic carbon storage capacity of the southern high-latitude/polar region. The study is also conducted in view of underpinning marine spatial planning and supporting conservation measures, present and future.

2. Materials and methods

2.1. Scotia Arc study areas and sites

Situated in the southern South Atlantic Ocean and Atlantic sector of the Southern Ocean, the four study areas, collectively making up the "study region", lie within the latitudinal and longitudinal ranges of ~53–67°S and ~37–71°W, respectively (Fig. 1A; Table 1). The study areas are ~760 to 2200 km apart and are connected by the underwater ridge and island system of the Scotia Arc, which links the Terra del Fuego region of South America to the Antarctic Peninsula and semi-

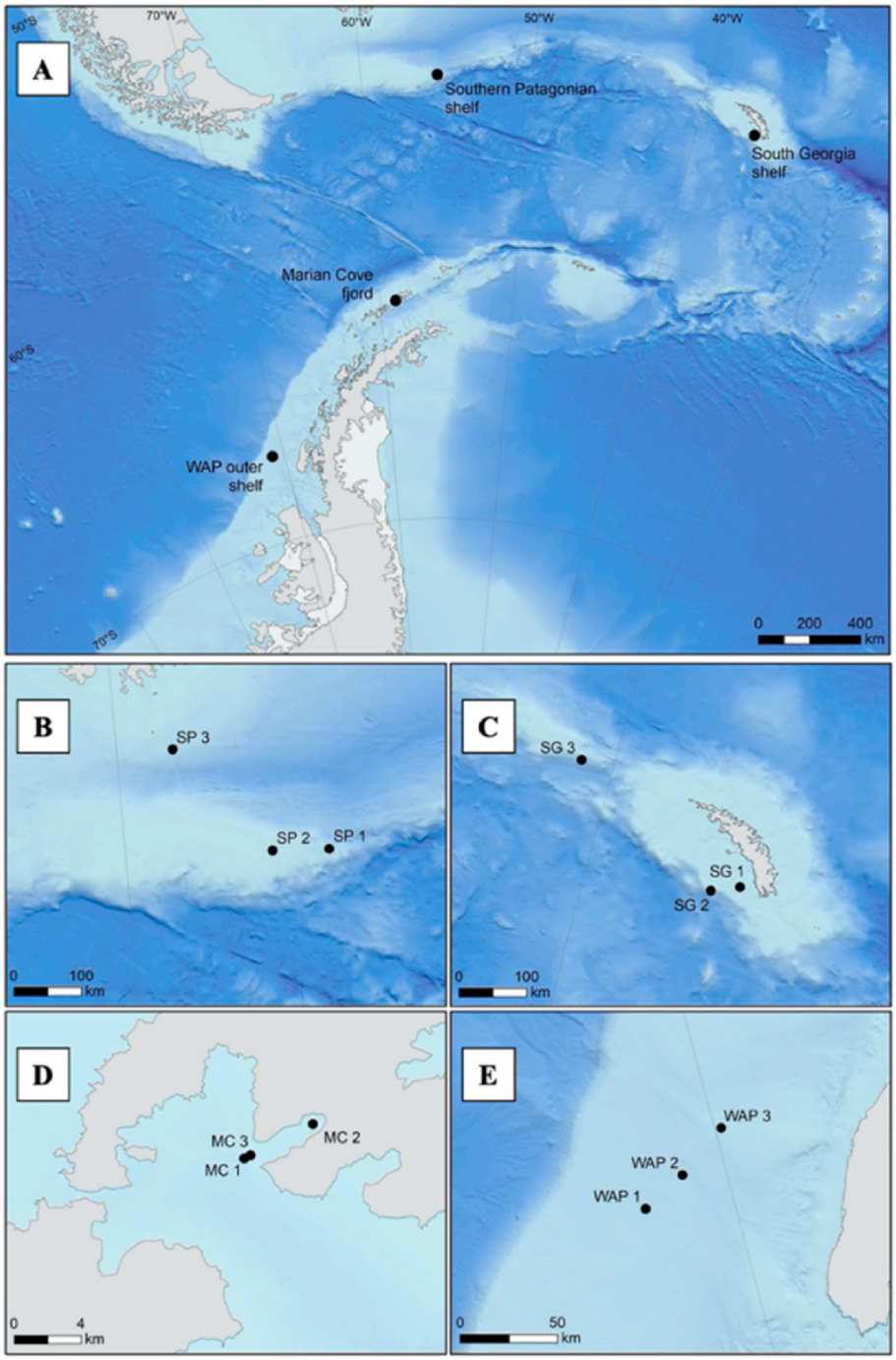

Fig. 1. Southern South Atlantic and Antarctic study areas and respective sites where benthic imagery was captured by the bespoke Shelf Underwater Camera System (SUCS). (**A**) Location of study areas in the wider context of the southern South Atlantic Ocean and Atlantic sector of the Southern Ocean, including the southern Patagonian shelf, South Georgia shelf, Marian Cove fjord (of King George Island), and the western Antarctic Peninsula (WAP) outer continental shelf; (**B**) Southern Patagonian shelf sites SP1-3; (**C**) South Georgia island shelf sites SG1-3; (**D**) Marian Cove fjord sites MC1-3; and (**E**) WAP outer continental shelf sites WAP1-3. White areas of the main map denote ice shelves, and grey areas of all maps represent land or ice-covered land/grounded ice (as appropriate). The bathymetry data is from the International Bathymetry Chart of the Southern Ocean v2 (Dorschel et al., 2022), with 100 m contours.

encloses the Scotia Sea. The northernmost study area falls within the southern South Atlantic Ocean and is situated on the southeast Patagonian shelf and the western side of the North Scotia Ridge. The most easterly study area is the shelf around the island of South Georgia, positioned south of the Polar Front, the strongest jet of the ACC, at a cusp between sub-Antarctic and Antarctic waters. Following the Scotia Arc clockwise from South Georgia toward higher latitudes leads to the third study area, Marian Cove (a relatively enclosed fjord basin) of King George Island – the largest island of the South Shetland Islands. This archipelago is at the southern boundary of the Drake Passage, and the study area is separated from the South Scotia Ridge and the Antarctic Peninsula by the Bransfield Strait. The fourth and most southerly study area is some 760 km from King George Island, situated west of Marguerite Bay and Adelaide Island on the outer continental shelf of the western Antarctic Peninsula in the Bellingshausen Sea, and falls within the Antarctic Circle. The study areas of the Scotia Arc study region are herein referred to as SP for southeast Patagonia, SG for South Georgia, MC for Marian Cove and WAP for the western Antarctic Peninsula.

Table 1
Southern South Atlantic and Antarctic study areas and sites, including latitude (∘S), longitude (∘W) and water depth (m) (all means across associated benthic imagery), and habitat type.

Study area	Site	Latitude[a]	Longitude[a]	Depth[a]	Habitat type
Southern Patagonian shelf	SP1	−54.4949	−55.5205	610	Shelf bank
	SP2	−54.4997	−56.7649	109	
	SP3	−53.1558	−58.8065	572	
South Georgia shelf	SG1	−54.8735	−36.5875	166	Shelf bank
	SG2	−55.0314	−37.1792	236	
	SG3	−53.7746	−40.6700	678	
Marian Cove (of King George Island)	MC1	−62.2200	−58.8159	205	Fjord
	MC2	−62.2031	−58.7313	83	
	MC3	−62.2174	−58.8065	62	
WAP outer continental shelf	WAP1	−66.9342	−71.0422	479	Trough
	WAP2	−66.7882	−70.4847	620	
	WAP3	−66.6648	−69.9220	358	

[a] Recorded during collection of benthic imagery by an underwater acoustic positioning system – all depths fall within the depth range of the Antarctic continental shelf (Clarke et al., 2004).

Each Scotia Arc study area was represented by three continental/island shelf sites (Fig. 1B–E; Table 1) with associated field datasets acquired during various ship-based, chiefly Royal Research Ship RRS *James Clark Ross*, scientific expeditions occurring during austral summers spanning 2009–2020. The southeast Patagonian shelf sites include two at the shallow seamount Burdwood Bank (~18,000 km^2 in area) lying ~200 km south of the Falkland Islands (Islas Malvinas); the sites correspond to SP1 and SP2 and are of ~610 and 110 m water depth, respectively. The third site, SP3 (~570 m depth), lies south of Beauchêne Island – the southernmost and most remote island of the Falkland archipelago at >60 km from East Falkland. At South Georgia, two sites are situated on the island's southern shelf, SG1 (at ~170 m depth) mid-shelf and SG2 (~240 m depth) at the shelf break, while SG3 (~680 m depth) is located on the western shelf of the island. At King George Island, the specific area of focus is Marian Cove fjord, bordered by the Weaver and Barton Peninsulas and situated within Maxwell Bay. With regard to Marian Cove sites, MC1 (at ~200 m depth) sits just outside the fjord (at the entrance), while MC2 (~80 m depth) lies deep within and is closest to the glacier terminus, and MC3 (~60 m depth) is located on the sill of the cove. On the outer continental shelf of the WAP, all three sites, WAP1-3, are situated westward of Marguerite Bay and Adelaide Island, with a depth range of ~360–620 m.

2.2. Environmental data collection

To determine how study sites and/or areas differed environmentally and to help identify environmental variables potentially responsible for biological structuring, various environmental datasets, collected in situ (during seabed imagery collection campaigns), remotely sensed and imagery-analysis-derived, were utilised.

In situ oceanographical data were acquired for each site (during corresponding imagery acquisition efforts) by deploying a Conductivity-Temperature-Depth system (CTD) fitted with auxiliary sensors. The CTD was cast from the sea surface to within ~10 m of the seabed, obtaining near-seafloor temperature (°C), salinity (Practical Salinity Unit; PSU), dissolved oxygen (O_2; μmol L^{-1}), chlorophyll-a (μg L^{-1}) and turbidity (beam transmittance; %) measurements.

Daily sea-ice concentration (SIC; %) data, spanning October 1978 to December 2021, and derived from passive microwave observations, were obtained from the US National Snow and Ice Data Center (NSIDC) (in conjunction with the US National Oceanic and Atmospheric Administration; NOAA). The dataset used was the NOAA/NSIDC Climate Data Record of Passive Microwave Sea Ice Concentration, Version 4 (G02202) (Meier et al., 2021), with a 25 by 25 km grid cell resolution. These records were used to calculate mean SIC for each site and area for the 14-year period prior to respective imagery collection (see section 2.3 regarding the latter), the period complementing available primary production data. As per Cummings et al. (2021), a year was considered as being from July through to June. In addition, the mean number of days sea-ice-covered per year was also computed for each site and area for the same period, with ≥85% sea-ice concentration/cover considered sea-ice-covered (as per Souster et al., 2020). For the purpose of the study, study sites were defined as "sea-ice sites" when the mean number of days of sea-ice-covered per year was at least 40.

Daily net primary production (NPP; mg C m^{-2} day^{-1}) data, spanning September 1997 to July 2019, were generated following the methods of Arrigo et al. (2008, 2015). From such data, mean daily NPP and mean peak NPP were calculated for each site and area for the 14-year period prior to respective imagery collection.

Daily sea surface temperature (SST; °C) data, spanning September 1981 to March 2022, were obtained from NOAA. The dataset used was the NOAA 1/4° Daily Optimum Interpolation Sea Surface Temperature dataset (Huang et al., 2020). From such data, mean daily SST was calculated for each site and area for the 14-year period prior to respective imagery collection, again the period complementing available primary production data.

Substratum type and rugosity of each image were determined during seafloor imagery analysis (section 2.4), and corresponding (mode-based) assignments assigned to each site.

2.3. Continental shelf imagery collection

Seabed imagery (for example images see Fig. S1) was acquired for each study site using the Shelf Underwater Camera System (SUCS; developed by the British Antarctic Survey Antarctic Marine Engineering Team). SUCS comprises a high-resolution still camera, lights, and a real-time ultra-short baseline positioning beacon, all mounted on a tethered (fibre-optic multimode cable) tripod, which can adjust for slope (see Barnes et al., 2020; Zwerschke et al., 2022). The camera was positioned perpendicular to the seabed at the same pre-set distance to capture images with a known field of view (area), enabling faunal density calculations. Images were captured when the tripod was at rest and spaced ~5 m apart to avoid spatial overlap. Typically, 20 images (replicates) were taken per site; hence, 60 per study area and ~240 across the Scotia Arc region.

2.4. Imagery analysis and functional group and VME indicator assignments

Each seafloor image collected was analysed for discernible zoobenthic macro- and mega-fauna using the web-based imagery annotation software BIIGLE 2.0 (www.biigle.de; Langenkämper et al., 2017). For each image, the number of different morphotaxa (morphotaxa richness) was recorded, and counts of individual functional groups (see Table 2; adapted from Barnes and Sands, 2017; Frinault et al., 2022) were conducted; hence, functional group richness was also recorded. Functional groups were based on mobility, feeding strategy and skeletal support (see Barnes and Sands, 2017) and included three suspension-feeding groups, three deposit-feeding groups, a flexible feeding strategy group (typified in the study by ophiuroids), a grazing group and five predating/scavenging groups. The number of taxa considered indicative of VMEs, as per CCAMLR (2009), was also determined (referred to herein as VME indicator taxa or simply VME taxa). As the area of each image was known, taxonomic group, functional group, and VME taxa counts could be converted into corresponding densities, i.e., individuals per m^2 (ind. m^{-2}) – standardisation permitting direct comparisons.

Additionally, for each image, substratum type was categorised as mud/fine sand, coarse sand, fine pebbles, coarse pebbles, cobbles, boulders/bedrock, or biogenic. The seven categories (principally of

Table 2
Functional groups based on Barnes and Sands (2017) and Frinault et al. (2022), with example taxa discerned in this study.

Functional group	Example taxa
Pioneer sessile suspension feeders	Ascidians, encrusting bryozoans, some tubicolous polychaetes
Climax sessile suspension feeders	Brachiopods, some erect bryozoans, poriferans (of classes Demospongiae and Hexactinellida)
Sedentary/mobile suspension feeders	Crinoids, some holothurians
Crawling (epi-faunal) deposit feeders	Holothurians
Soft (in-faunal) deposit feeders	Echiurans, some polychaetes, sipunculans
Hard (burrowing) deposit feeders	Bivalves, irregular echinoids, scaphopods
Flexible strategists	Ophiuroids
Grazers	Regular echinoids, gastropods
Soft sessile predator/ scavengers	Actiniarians, hydroids, pennatulaceans, soft corals, staurozoans
Hard sessile predator/ scavengers	Calcaxonian whips, hydrocorals, scleractinians
Soft mobile predator/ scavengers	Octopi, nemerteans, nudibranchs
Hard mobile predator/ scavengers	Asteroids, fish, some gastropods
Arthropod predator/ scavengers	Amphipods, decapod shrimps, pycnogonids

increasing sediment grain size) were based on the modified Udden-Wentworth sediment classification scheme (Blair and McPherson, 1999) and categorisations by Barnes et al. (2019) and Souster et al. (2020). Further to substratum categorisation, an image was also defined as a "dropstone image" if a dropstone or boulder was present at least three sediment-size classes larger than proximate substrata (for more information regarding glacial dropstones, see Ziegler et al., 2017; Post et al., 2020) in order to assess if such features had any influence on zoobenthic carbon storage and other biological variables in the study region. Finally, rugosity, the small-scale roughness of the seabed, was graded by measuring the "shadow length" of substrata (again following Barnes et al., 2019; Souster et al., 2020). The seven categories (of increasing rugosity) included <1 mm (i.e., smooth), 1–10 mm, >10–20 mm, >20–30 mm, >30–40 mm, >40–50 mm and ≥50 mm (i.e., rough).

2.5. Zoobenthos – acquisition and carbon content analysis, and zoobenthic carbon storage estimations

Zoobenthic specimens were collected in the vicinity of SUCS deployments (and oceanographical data collections) using Agassiz or mini-Agassiz trawls. Specimens were washed and morphologically-identified prior to storage, with the carbon contents of identified taxa later determined and used to calculate the mean carbon content of each functional group for each study area. The total number of specimens used in such calculations varied from 84 to 102 per study area. For three study areas, zoobenthic carbon content data of associated specimens were acquired from previous studies, which employed identical methodologies (Barnes, 2017; Barnes and Sands, 2017; Bax, *pers. comms.*), and for Marian Cove, the carbon content of respective zoobenthos was determined as part of this study, with associated methods reported below.

The carbon content of Marian Cove zoobenthic specimens was determined following standardised methods (see Barnes, 2017; Barnes and Sands, 2017; Barnes et al., 2019; Souster et al., 2020), facilitating direct comparability. Specimens were first washed with deionised water (Millipore Elix® Type 2) and placed into pre-etched and pre-weighed aluminium weighing boats for the duration of the analysis; a specimen was divided between more boats as necessary. Specimens were then dried for 12–24 h in a drying oven (Genlab OV/125/F/DIG) at 70 °C until constant mass achieved and subsequently incinerated for 12 h in a muffle furnace (Carbolite ESF 12/10) at 480 °C and reweighed – the tissue mass, equivalent to ash-free dry mass (AFDM), having been burnt off and skeletal mass isolated. The organic carbon content of a specimen, C_{org}, was calculated as 50% of AFDM, while the inorganic carbon content, C_{inorg}, was computed as 12% of the residual skeletal mass; however, if a specimen was siliceous (e.g., a Hexactinellid sponge), C_{inorg} was calculated as 1% of the residual skeletal mass (as per Barnes and Sands, 2017). A specimen's total carbon content, C_{tot}, i.e., g of C held, was obtained by summing the corresponding values of C_{org} and C_{inorg}.

Using C_{tot} of all corresponding specimens, the mean C_{tot} of each functional group was computed for each study area – note, the mean C_{tot} a functional group will be influenced by which specimens are (able to be) collected. To estimate zoobenthic carbon storage per m^2 (C_{zoo}; g C m^{-2}), functional group densities, determined during section 2.4 procedures, were multiplied by respective values for mean C_{tot}. Around 20 separate C_{zoo} values were generated per study site, thus 60 for each study area.

2.6. Statistical analyses

Differences in C_{zoo} and faunal density among study areas were tested using non-parametric (Kruskal Wallis) tests (with Dunn's post-hoc tests) as associated data did not meet the assumptions of Analysis of Variance (ANOVA), even after transformation. The relationship between C_{zoo} and various biological variables (i.e., richness and density) was explored via linear regression.

In advance of multivariate analyses, performed in PRIMER v7 (Clarke and Gorley, 2015) with PERMANOVA + add-on (Anderson et al., 2008), and following established procedures (Clarke et al., 2014; Clarke and Gorley, 2015), all environmental/abiotic variables were assessed for collinearity (via Draftsman plots and an accompanying correlation matrix). For variables exhibiting a high correlation coefficient, r ≥ 95%, a single variable was retained as a proxy for the other (Table S1); the remaining variables were then normalised onto a common dimensionless scale for analysis. Biological data, i.e., functional group densities (assemblage structure) and C_{zoo} values split by functional group (carbon storage structure), were fourth-root transformed, permitting rarer/less numerically dominant groups to have some influence in subsequent similarity calculations (Clarke and Green, 1988).

The similarity between study sites' biological structuring was investigated using the Bray-Curtis similarity coefficient (which generates a resemblance matrix; Bray and Curtis, 1957), followed by hierarchical agglomerative cluster (HAC) analysis (based on the resemblance matrix; Everitt, 1980), with a similarity profile (SIMPROF) test (Clarke et al., 2008), and the similarity percentages (SIMPER) procedure (see Clarke, 1993).

The BEST (Bio-Env) routine, employing the Spearman's rank correlation coefficient, was used to identify which subset of environmental variables (Table S1) best matched, or "explained", the biological structuring observed, accompanied by a global BEST test (999 random permutations) to determine the statistical significance of the match (Clarke et al., 2008; Clarke and Ainsworth, 1993). The BEST routine uses biological resemblance and normalised-environmental data matrices (and applies Euclidean distance to the latter during the process). Total C_{zoo} was also explored as a single response variable, with the corresponding resemblance matrix being based on Euclidean distance (Clarke and Gorley, 2015).

In addition, Wilcoxon matched-pair signed-rank tests were used to compare the means of several biological variables of dropstone images and randomly-selected non-dropstone images (paired from the same study site).

3. Results

3.1. Environmental differences of study areas

In terms of CTD-derived environmental (i.e., in situ oceanographical) differences, and for SP, SG, MC and WAP collectively, mean (±1 SD) near-seafloor temperature (°C) ranged from 0.1 (±0.2) to 7.4 (±0.1); salinity (PSU) from 33.4 (±1.2) to 34.7 (±0.0); dissolved oxygen (μmol L^{-1}) from 177.8 (±6.3) to 346.6 (±19.8); chlorophyll-a (μg L^{-1}) from 0.02 (±<0.1) to 0.21 (±0.1); and turbidity (beam transmittance; %) from 93.8 (±2.3) to 97.9 (±0.3).

From remotely-sensed data, it was found that mean (±1 SD) SIC (%) for the 14-year period prior to respective imagery collection ranged from 0 (for SP) and 39.8 (±1.4) (for WAP). The mean (±1 SD) number of days per annum sea-ice-covered (days) varied from 0 (for SP and SG) to 117.4 (±7.4) (for WAP).

Mean daily and peak NPP for the 14-year period prior to respective imagery collection were highest at WAP and SP, respectively. For SP, SG, MC and WAP collectively, mean (±1 SD) daily NPP values (mg C m^{-2} d^{-1}) ranged from 300.3 (±0.2) to 389.3 (±36.5), and mean (±1 SD) peak NPP values (mg C m^{-2} d^{-1}) from 520.4 (±0.9) to 1126.8 (±548.4).

Mean (±1 SD) sea surface temperature (°C) for the 14-year period prior to respective imagery collection ranged from 5.8 (±0.4) (for SP) to −0.8 (±0.0) (for WAP).

Study area-specific means of environmental data can be found in Table S2.

Regarding imagery-informed environmental differences, the finest sedimented (i.e., mud/fine sand) and smoothest seabed (i.e., lowest rugosity) was observed at sites MC2, WAP2 and WAP3. The site with the coarsest sediment (largest grain size) and highest rugosity was SP3, which featured boulders. Coarse pebbles were observed at SG3 and WAP3.

3.2. Zoobenthos of the Scotia Arc imagery

Over 9400 individual fauna were detected across the Scotia Arc imagery, with all functional groups (Table 2) being represented. Overall, images were dominated by pioneer sessile suspension feeders (e.g., ascidians and encrusting bryozoans) and mobile flexible-feeding ophiuroids. Specifically, 39.4% of individuals belonged to the pioneer sessile suspension feeder group, 25.7% to the flexible feeding strategy group, 11.9% to the climax sessile suspension feeder group, which included, for example, demosponges, and 7.3% to the soft sessile predator/scavenger group (exemplified by sea anemones and hydroids) – the remaining individuals were distributed across the nine other functional groups. In addition, 46.8% of all zoobenthic taxa observed were classified as VME taxa, i.e., >4400 individuals.

3.3. Zoobenthic carbon storage across study areas

A zoobenthic specimen of the Scotia Arc study region held, on average, 0.3 g of carbon (with a standard deviation of ±0.6). When looking at the mean (±1 SD) C_{tot} of individual functional groups across all study areas, 0.001 (±0.0007) g was the lowest value calculated (the responsible functional group type being crawling deposit feeders – i.e., holothurians) and 2.1 (±2.3) g the highest (the responsible functional group types being soft mobile predator/scavengers) (see Fig. S2). The mean C_{tot} of a particular functional group varied between the four study areas. Considering all respective specimens, mean C_{tot} was lowest for SG (which bisects the ACC), followed by SP and MC, and highest for WAP.

At site level, means (plus standard deviations) for zoobenthic carbon storage ranged from 2.4 (±2.5) g C m^{-2} at SP1 to 76.0 (±39.4) g C m^{-2} at WAP3. At study area level, means for zoobenthic carbon storage were 8.2 (±8.9), 6.2 (±5.1), 38.6 (±28.8), and 44.6 (±57.9) g C m^{-2} for SP, SG, MC, and WAP, respectively, i.e., the two polar study areas south of the ACC exhibited higher mean carbon storage values compared to the other two areas, collectively averaging 41.6 (±45.6) and 7.2 (±7.3) g C m^{-2}, respectively. Kruskal Wallis tests indicated that all study areas significantly differed in terms of carbon storage except the two lower-latitude areas, SP and SG (Table 3).

3.4. Zoobenthic carbon storage and morphotaxa and functional group richness

An objective of the current study was to investigate relationships between marine biological carbon storage and biodiversity measures (morphotaxa and functional group richness). For all study areas, statistically significant positive relationships were found between zoobenthic carbon storage and morphotaxa richness; however, some relationships appeared stronger than others, in particular, those of SP and WAP (see Fig. 2A) – the most northerly and southerly areas, respectively. Thus, it appeared that greater carbon storage function, within the study region, generally aligned with higher biodiversity (richness). In addition, the carbon-morphotaxa richness relationships of the study areas were all statistically significantly different.

Significant positive relationships were also found between C_{zoo} and functional group richness (Fig. 2B); however, these relationships were not as strong as those observed for C_{zoo} and morphotaxa richness. WAP exhibited the strongest relationship of all areas. Nonetheless, almost all carbon-functional group richness relationships were statistically significantly different, with the relationship of SP and SG the exception (i.e., not significantly different).

3.5. Faunal density and zoobenthic carbon storage

In terms of seabed macro- and mega-faunal densities, WAP exhibited the highest image level faunal density value, 484.9 ind. m^{-2}, and also the highest estimated zoobenthic carbon storage value, 297.5 g C m^{-2} (Fig. 3). When examining lowest faunal densities, some images had no discernible fauna, i.e., faunal densities of zero (including imagery of sites SG2, WAP1 and WAP2). The lowest density greater than zero was observed in an SP1 image at 2.5 ind. m^{-2}. At site level, the highest mean faunal density was 255.1 (±88.4) ind. m^{-2} at WAP3, and the lowest was 12.8 (±2.4) ind. m^{-2} at SP1 – the former aligning with the highest average for carbon storage and the latter aligning with the lowest average for carbon storage (see 3.3). Kruskal Wallis tests indicated that SP statistically significantly differed from all other study areas in terms of faunal density, while SG and MC, SG and WAP, and MC and WAP did not significantly differ (see bottom row of Table 3).

For all study areas, significant positive relationships were found between zoobenthic carbon storage and faunal density, and carbon-faunal density relationships were all statistically significantly different (Fig. 3). Generally, C_{zoo} exhibited a stronger relationship with faunal density than with morphotaxa and functional group richness; the exception being WAP, where the carbon-morphotaxa richness relationship appeared the strongest of the relationships examined.

3.6. VME taxa and zoobenthic carbon storage

VME taxa contributed at least 53% to zoobenthic carbon storage at eight (out of 12) study sites. In the SP study area, VME taxa contributed 81, 87 and 31% at sites SP1-3, respectively; hence, VME taxa contribution to zoobenthic carbon storage was highest at the two Burdwood Bank sites, corresponding with previous observations (Bax, *pers. comms.*). For the SG study area, SG3 (situated on the western shelf) exhibited the highest VME taxa contribution at 56%, while contributions at SG1 and SG2 (both on the southern shelf) were lower at 23 and 7%, respectively. In MC, VME taxa contributions to zoobenthic carbon storage were high across study sites at 53, 82 and 66% for MC1-3, respectively. Finally, VME taxa contributed 86, 31 and 64% at WAP1-3, respectively. Overall, WAP1 (the southernmost site of the study) displayed the highest site-level VME taxa contribution to zoobenthic

Table 3
P-values (with Bonferroni correction) resulting from Kruskal-Wallis tests between Scotia Arc study areas for zoobenthic carbon storage (C_{zoo}; g C m^{-2}) and faunal density (ind. m^{-2}). Regarding continental/island shelf study areas: SP = South Patagonia (specifically the shelf of the Falkland Islands/Islas Malvinas); SG = South Georgia; MC = Marian Cove (of King George Island); and WAP = western Antarctic Peninsula (westward of Marguerite Bay and Adelaide Island). Significant p-values are shown in bold and asterisked.

	SP vs SG	SP vs MC	SP vs WAP	SG vs MC	SG vs WAP	MC vs WAP
C_{zoo}	$p > 0.05$	**$p < 0.001$****	**$p < 0.001$****	**$p < 0.001$****	**$p < 0.001$****	**$p = 0.049$***
Faunal density	***p < 0.001*****	***p < 0.001*****	***p < 0.001*****	*p > 0.05*	*p > 0.05*	*p > 0.05*

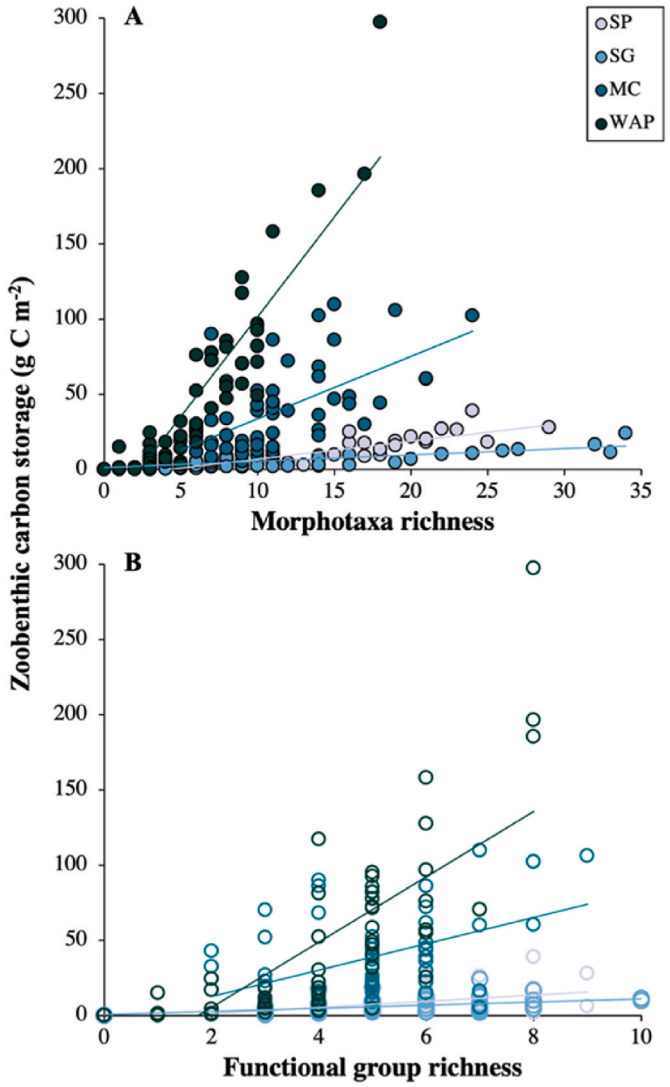

Fig. 2. Carbon storage by zoobenthos (C_{zoo}; g C m^{-2}) versus faunal richness for (**A**) morphotaxa richness and (**B**) functional group richness. R^2 for (**A**): SP = 0.82; SG = 0.42; MC = 0.35; and WAP = 0.82. R^2 for (**B**): SP = 0.19; SG = 0.21; MC = 0.19; and WAP = 0.53. Regarding continental/island shelf study areas: SP = South Patagonia (specifically the shelf of the Falkland Islands/Islas Malvinas); SG = South Georgia; MC = Marian Cove (of King George Island); and WAP = western Antarctic Peninsula (westward of Marguerite Bay and Adelaide Island). For C_{zoo} versus morphotaxa richness, all slopes were statistically significantly different (p-values all <0.001). For C_{zoo} versus functional group richness, all slopes were significantly different (p-values all <0.001, bar SP versus MC, where the p-value was 0.004) except for SP versus SG, where the p-value was non-significant. Regression-associated ANOVA results for C_{zoo} versus morphotaxa richness: F = 258.33, 39.85, 31.69, and 267.30 for SP, SG, MC, and WAP, respectively, and p-values all <0.001, and for C_{zoo} versus functional group richness: F = 12.84, 13.33, 15.76, and 78.87 for SP, SG, MC, and WAP, respectively, and p-values all <0.001.

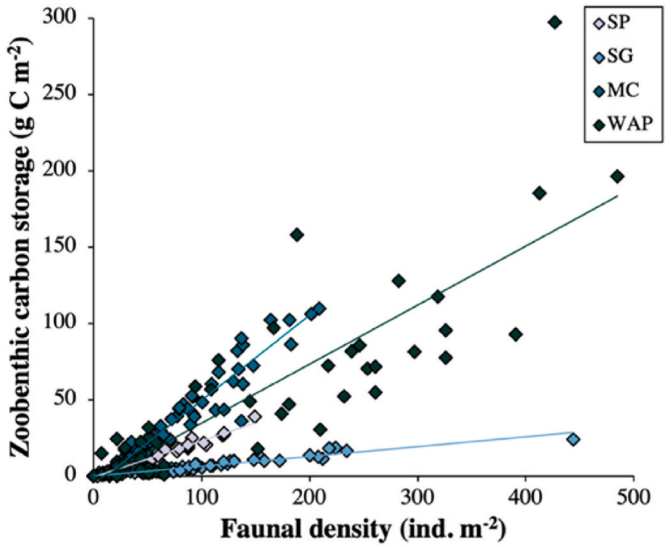

Fig. 3. Carbon storage by zoobenthos (C_{zoo}; g C m^{-2}) versus faunal density (ind. m^{-2}). R^2: SP = 0.97; SG = 0.92; MC = 0.92; and WAP = 0.75. Regarding continental/island shelf study areas: SP = South Patagonia (specifically the shelf of the Falkland Islands/Islas Malvinas); SG = South Georgia; MC = Marian Cove (of King George Island); and WAP = western Antarctic Peninsula (westward of Marguerite Bay and Adelaide Island). All slopes were statistically significantly different (p-values all <0.001). Regression-associated ANOVA results for C_{zoo} versus fauna density: F = 1874.79, 672.35, 639.96, and 172.68 for SP, SG, MC, and WAP, respectively, and p-values all <0.001.

carbon storage of all sites, and SG2 the lowest.

In addition, the relationship between zoobenthic carbon storage and VME taxa density was also examined for each study area (Fig. 4). All carbon-VME density relationships were positive and significant and significantly differed from one another. Compared to carbon and complete faunal density relationships (Fig. 3), the carbon-VME density relationships displayed slightly lower R^2 and less significant p-values for SP and MC, and a much lower R^2 and less significant p-value for SG; however, a higher R^2 and more significant p-value for WAP.

3.7. Functional group contributions to zoobenthic carbon storage and faunal density

Overall, nine functional groups were found to be substantial contributors (i.e., ≥10%) to zoobenthic carbon storage at site level (Fig. 5), the exceptions being sedentary/mobile suspension feeders and all deposit-feeding groups. At area level, six functional groups were substantial contributors (see Fig. S3), including pioneer sessile suspension feeders, climax sessile suspension feeders, grazers, soft and hard sessile predator/scavengers, and flexible strategists. No individual functional group was found to be a substantial contributor to zoobenthic carbon storage at all 12 sites, and similarly, no individual group was found to be a major contributor in all four study areas.

Functional groups which contributed most substantially to the zoobenthic carbon stored at each study area (Fig. S3) included climax sessile suspension feeders at both SP and WAP (49.0 and 50.5%, respectively),

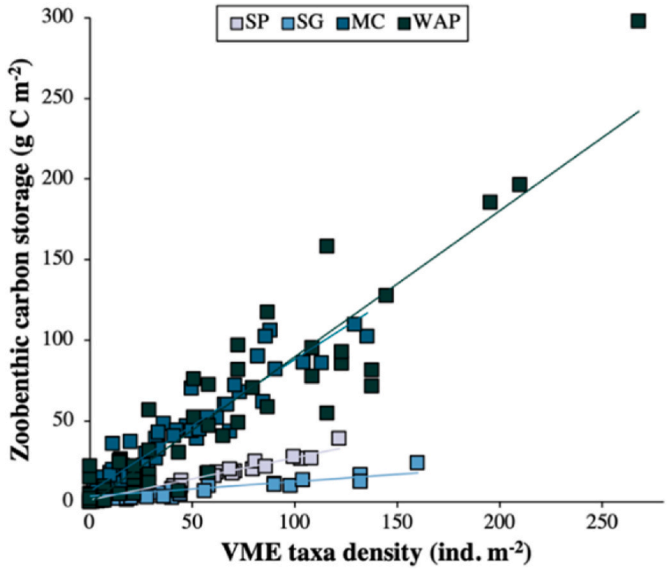

Fig. 4. Zoobenthic carbon storage (C_{zoo}; g C m^{-2}) versus density of Vulnerable Marine Ecosystem (VME) indicator taxa (ind. m^{-2}). R^2: SP = 0.96; SG = 0.40; MC = 0.90; and WAP = 0.87. Regarding continental/island shelf areas: SP = South Patagonia (specifically the shelf of the Falkland Islands/Islas Malvinas); SG = South Georgia; MC = Marian Cove (of King George Island); and WAP = western Antarctic Peninsula (westward of Marguerite Bay and Adelaide Island). All slopes were statistically significantly different (p-values all <0.001). Regression-associated ANOVA results for C_{zoo} versus VME taxa density: F = 1289.91, 37.17, 498.79, and 404.72 for SP, SG, MC, and WAP, respectively, and p-values all <0.001.

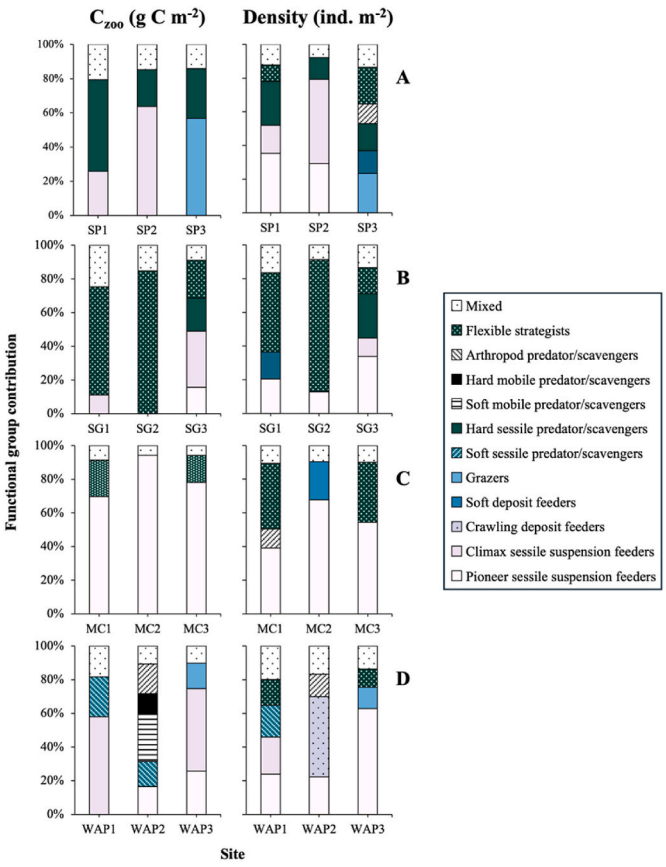

Fig. 5. Average functional group contribution (%) to zoobenthic carbon storage (C_{zoo}; g C m^{-2}) and faunal density (ind. m^{-2}) for continental/island shelf study sites of (**A**) South Patagonia (specifically the shelf of the Falkland Islands/Islas Malvinas), (**B**) South Georgia, (**C**) Marian Cove (of King George Island), and (**D**) the western Antarctic Peninsula (westward of Marguerite Bay and Adelaide Island). Individual functional groups are shown where their contribution was ≥10%. Otherwise, groups were pooled with others whose contributions were also <10% and designated as the "mixed" group.

flexible strategists (i.e., ophiuroids) at SG (54.9%), and pioneer sessile suspensions feeders at MC (80.7%). Other substantial contributors to zoobenthic carbon storage included hard sessile predator/scavengers and grazers at SP, climax sessile suspension feeders and pioneer sessile suspension feeders at SG, flexible strategists at MC, and pioneer sessile suspension feeders and soft sessile predator/scavengers at WAP. The "mixed" group, which included functional groups that individually contributed <10% to zoobenthic carbon storage, also substantially contributed in three out of four study areas (ranging from 13.1 to 20.8%), the exception being MC (at 6.4%).

At a more granular level (i.e., site level; Fig. 5), different combinations of functional groups substantially contributed to zoobenthic carbon storage. For example, functional groups substantially contributing at SP sites included hard sessile predator/scavengers at SP1-3 (53.6, 21.7, and 29.8%, respectively), climax sessile suspension feeders at SP1 and SP2 (25.9 and 63.7%, respectively), and grazers (made up of grazing gastropod molluscs), rather than climax sessile suspension feeders, at SP3 (56.7%). At SG1, flexible strategists (64.3%) and climax sessile suspension feeders (11.1%) were substantial contributors, as well as the mixed group (24.6%). At SG2, flexible strategists were the dominant carbon storage contributors (84.8%), the remaining contributors all within the mixed group (15.2%). At SG3, four individual functional groups substantially contributed to zoobenthic carbon storage: flexible strategists (22.5%; as observed at SG1 and SG2), climax sessile suspension feeders (33.2%; and consistent with SG1), and, in addition, hard sessile predator/scavengers (19.8%) and pioneer sessile suspension feeders (15.7%). The most considerable contribution to zoobenthic carbon storage at MC1-3 was from the pioneer sessile suspension feeders functional group (with a percentage contribution range of 69.7–94.2%), and, at MC1 and MC3, a substantial contribution was also observed from flexible strategists (21.8 and 16.0%, respectively). The mixed group did not contribute substantially at any MC site (all ≤8.5%). At both WAP1 and WAP3, climax sessile suspension feeders were the major contributor to carbon storage (at 58.0 and 48.9%, respectively), although not at WAP2. Site WAP2 appeared to be the most complex with respect to major contributor make-up, with five functional groups substantially contributing to zoobenthic carbon; groups included soft sessile predator/scavengers (in common with WAP1), pioneer sessile suspension feeders (in common with WAP3) and, additionally (and contrary to WAP1 and WAP3), soft mobile predator/scavengers (27.9%), arthropod predator/scavengers (17.5%), and hard mobile predator/scavengers (12.4%).

Across the study region, at both study area and site level, functional group (percentage) contributions to zoobenthic carbon storage differed from respective contributions to faunal density (see Fig. 5 and S3, respectively). For example, at area level, some functional groups had greater contributions to C_{zoo} than density, e.g., climax sessile suspension feeders at SP, SG and WAP, grazers and hard sessile predator/scavengers at SP, flexible strategists at SG, pioneer sessile suspension feeders at MC, and soft sessile predator/scavengers at WAP. Conversely, some functional groups had smaller contributions to C_{zoo} than density, including pioneer sessile suspension feeders at SP, SG, and WAP, soft sessile predator/scavengers at SG, and hard sessile predator/scavengers at MC and WAP (the two south of 60°S polar areas). This observation was similarly the case for site-level functional group percentage contributions (Fig. 5), where some functional groups contributed greatly to C_{zoo} and not faunal density, and vice versa.

3.8. Assemblage and zoobenthic carbon storage structures and potential environmental drivers

With regard to assemblage structure (by functional groups), HAC analysis (with SIMPROF) identified four distinct groupings among the 12 sites (Fig. S4A). WAP2, MC2 and SP3 were each compositionally distinct (hence, each their own group), while the remaining nine sites formed one group (with an average similarity of 75.6% and with pioneer sessile suspension feeders, flexible strategists and climax sessile suspension feeders being the top functional groups contributing to similarity [according to SIMPER]). WAP2 and the group comprising the nine sites were the most compositionally dissimilar (with an average dissimilarity of >44% – principally due to an abundance of crawling deposit feeders and a lack of climax sessile suspension feeders and hard sessile predator/scavengers at WAP2). For more details, see Table S3.

Regarding carbon storage (by functional group) structure, HAC analysis (with SIMPROF) identified six distinct groupings among sites (Fig. S4B). MC2 and WAP2 constituted one group, which had the lowest average similarity at 59.7%, SP3 was compositionally distinct in its own right (hence, its own group), WAP1 and WAP3 formed another group, SP1 and SP2 another, and SG1-3, MC1 and MC3 the final group (with an average similarity of 74.2%). The MC2 and WAP2 group (both polar sites) and the SP1-2 group (the northernmost sites) were the most compositionally dissimilar (with an average dissimilarity of 54.7%). For the SP1-2 group and the MC2 and WAP2 group, dissimilarities were principally driven by hard sessile predator/scavengers, climax sessile suspensions feeders, pioneer sessile suspension feeders, and in-faunal deposit feeders. For more details, see Table S4.

BEST analyses indicated that a subset of four environmental variables most highly correlated with the variation in faunal assemblage structure (by functional groups) (Rho correlation = 0.34, p-value <0.01). The subset comprised sea-ice cover, peak NPP, turbidity, and substratum.

For the carbon storage by functional group data, a subset of three environmental variables was identified as the most highly correlating (Rho correlation = 0.41, p-value <0.01). The subset included sea-ice cover, peak NPP, and temperature.

Sea-ice cover was the single variable with the highest correlation with assemblage and carbon storage by functional groups structures (Rho correlations all >0.32), and sea-ice cover and peak NPP were encompassed in all optimal subsets of environmental variables. The subsets, therefore, included a mixture of remotely sensed and local-scale environmental variables.

Additionally, when examining zoobenthic carbon storage as a single response variable, sea-ice cover was both the single variable with the highest correlation and the optimal subset (Rho correlation = 0.26, p-value <0.01).

3.9. Influence of dropstones

The influence of dropstones and boulders (relatively raised physical seabed features) on zoobenthic carbon storage and other biological variables was also examined. All dropstones observed were of boulder grain sizes (i.e., >256 mm; Blair and McPherson, 1999). Dropstone images, although relatively rare, representing just 3% of the Scotia Arc imagery analysed, displayed higher values (means) than non-dropstone images for all biological variables explored, i.e., morphotaxa and functional group richness, zoobenthic carbon storage and faunal density; however, Wilcoxon matched-pair signed-rank tests revealed these differences to be statistically non-significant (Table 4) – perhaps due to the limited sample size. SP1, SP2, SG3, MC1-3, and WAP3 each presented paired samples.

Table 4
Results of Wilcoxon matched-pair signed-rank tests for various biological variables of dropstone images and non-dropstone images of Scotia Arc continental/island shelf study areas. "N" indicates sample size (i.e., number of images) and the biological variables examined included morphotaxa and functional group richness, zoobenthic carbon storage (C_{zoo}; g C m^{-2}), and faunal density (ind. m^{-2}).

	Dropstone images $\bar{x}$ (±1 SD) N = 7	Non-dropstone images $\bar{x}$ (±1 SD) N = 7	Wilcoxon matched-pair test results
Morphotaxa richness	18.9 (±7.5)	11.3 (±5.3)	**p = 0.06**
Functional group richness	6.0 (±1.3)	5.0 (±1.3)	**p = 0.07**
Zoobenthic carbon storage	61.1 (±66.1)	30.1 (±44.1)	**p = 0.06**
Faunal density	191.8 (±190.3)	84.1 (±94.0)	**p = 0.09**

4. Discussion

The Scotia Arc study region, which encompasses the southern South Atlantic Ocean and Atlantic sector of the Southern Ocean, is a collective hotspot of climate change, high-latitude biodiversity, and ecosystem services; however, not, as of yet, protection (Rogers et al., 2020; Cavanagh et al., 2021). Much of the study region falls within a proposed network of marine protected areas (MPAs under consideration by CCAMLR (Brooks et al., 2020). Building evidence bases, such as those concerning biodiversity and blue carbon (as an ecosystem service), and VME taxa presence and their contributions to the former, is vital in supporting MPA designations; the current study contributes to such evidence bases. Additionally a recent review, supported by the Intergovernmental Panel on Climate Change, has recommended a synergistic approach to alleviating the biodiversity and climate crises (i.e., Pörtner et al., 2023). Although such an approach is seemingly yet to be implemented in polar waters, evidence is building, including from this study, with regard to high-latitude benthic biodiversity supporting carbon storage, and potentially climate change mitigation (Morley et al., 2022; Zwerschke et al., 2022; Sands et al., 2023).

4.1. Variation in zoobenthic carbon storage

Reflecting the complex and patchy nature of southern high-latitude continental/island shelf habitats, zoobenthic carbon storage was here found to vary within and between study sites and study areas – i.e., over different spatial scales. Nonetheless, when comparing the combined average for carbon storage by zoobenthic assemblages of the two southernmost study areas with that of the two northernmost areas, the former was six times greater than that of the latter. This considerable difference in ecosystem function could be for several reasons, including, for example, the two areas south of the ACC being comparatively less disturbed, naturally and/or anthropogenically; both areas experience periods of sea-ice cover, which can afford protection from various physical disturbances such as iceberg scouring (Smale et al., 2008; Clark et al., 2017). In addition, some sites, such as WAP1-2 of the Bellingshausen Sea, are also situated at depths beyond the reach of many modern iceberg keels (Dowdeswell and Bamber, 2007); thus, should evade most ice scouring. This attribute, however, is not shared by WAP3 (the respective site exhibiting the highest zoobenthic carbon storage and faunal density values), which is at a depth of 358 m, and hence, at greater risk of experiencing iceberg-mediated disturbance. Nevertheless, areas with more constant environmental conditions (e.g., deprived of or with minimal disturbance) could promote the development/advancement of benthic communities to later (more complex) successional stages (Teixidó et al., 2007) with potentially positive implications for carbon storage capacity (Barnes et al., 2020). Furthermore, in (seasonally) sea-ice covered areas, sympagic (ice-affiliated) primary production can also be taking place, with the organic matter produced principally reaching and consumed by the benthos (Cautain et al., 2022).

4.2. Extrapolating zoobenthic carbon storage to the antarctic continental shelf

In blue carbon studies, findings are occasionally extrapolated to a wider region/environment (e.g., Barnes et al., 2019, 2020; Sands et al., 2023). For the current study, an extrapolation is made for the Antarctic continental shelf, which is deep (up to 1000 m) and extensive, constituting an area of 4.6 million km^2 (Clarke and Johnston, 2003). However, as around one-third of the Antarctic continental shelf is overlain by ice shelves, floating seaward extensions of the Antarctic Ice Sheet, and very little is known about or documented for the benthic assemblages residing beneath ice shelves, for example, compositional, functional or behavioural traits (see Barnes et al., 2021b; Griffiths et al., 2021; Frinault et al., 2023), this study's extrapolation extends the ice-shelf-free continental shelf only. Based on mean zoobenthic carbon storage from MC and WAP data (south of the ACC), it is therefore estimated that ~125 million tonnes of carbon could be stored on the open-water continental shelf by epi-zoobenthic assemblages alone. This estimate, although conjectural, is equivalent to a CO_2 drawdown of 458 million tonnes, which, for contextualisation purposes only, is a greater amount than the CO_2 (including equivalents) estimated to have been emitted by the United Kingdom in 2022 (DESNZ, 2023). If in-faunal benthic carbon storage were to be included in the appraisal, the amount of carbon stored in Antarctic open shelf benthos, and equivalent GHG drawdown, is potentially considerably higher (e.g., see Zwerschke et al., 2022). Such extrapolations should, nonetheless, be treated with caution, especially in Antarctica, given the innate heterogeneous and patchy nature of its seabed habitats and communities – some areas of the continental shelf appear depauperate while others are highly abundant and biodiverse (Post et al., 2017; Almond et al., 2021; Brasier et al., 2021). Although, in this study, the highest latitude areas of interest already displayed the highest estimated zoobenthic carbon storage values per unit area, it is thought that the capacity of Antarctica's continental shelf to store carbon will, in the absence of disturbance, e.g., from fishery activities, increase with loss of ice cover – potentially acting as a negative feedback on climate change (Peck et al., 2010; Barnes et al., 2020; Morley et al., 2022; Zwerschke et al., 2022; Sands et al., 2023).

4.3. Zoobenthic carbon storage aligns with richness and faunal density

The climate change crisis is considered intertwined with the dilapidation of ecosystems, and the ongoing biodiversity crisis, hence, the degradation or forfeiture of associated functions (IPCC, 2022, 2023; Pörtner et al., 2023; Siegert et al., 2023). Marine ecosystems that can be identified as assisting with moderating climate change (e.g., through their carbon storage capacity), by virtue of hosting diverse biological communities, could be prioritised for protection in marine spatial planning to help address these entangled issues. A key objective of the current study, therefore, was to ascertain whether zoobenthic carbon storage variance aligns with biodiversity measures (richness), and also faunal density. For all study areas, zoobenthic carbon storage increased with richness (biodiversity), particularly morphotaxa richness. Thus, species-rich or carbon-rich areas could be priority areas for protection (permitting both bio/ecological elements to be protected simultaneously). For each area, zoobenthic carbon storage also exhibited a particularly strong relationship with density. Such an alignment has been observed elsewhere, including in the Barents Sea, in the northern hemisphere (Souster et al., 2020), and on the South Georgia shelf (see Fig. 2 of Barnes and Sands, 2017), and potentially indicates that ecosystem monitoring and MPA efficacy evaluations could be supported by higher-level data.

4.4. VME taxa prevalent and major contributors to zoobenthic carbon storage

In the Southern Ocean, seabed conservation and management tools include an array of benthic taxa classified by CCAMLR as VME indicators (CCAMLR, 2009; FAO, 2009). While the approach can be important for decision-making, e.g., regarding CCAMLR MPA design and designation, it is not yet fully known whether all such taxa indicate VMEs or, indeed, are vulnerable themselves (see Dayton et al., 2013, 2016; Fillinger et al., 2013). However, advances are being made to better characterise the vulnerability of these taxa based on morphology (Gros et al., 2023). The current study importantly has shown that VME indicator taxa are both prevalent components of benthic assemblages observed, particularly those assemblages of Burdwood Bank (and polar site WAP1), and major contributors to zoobenthic carbon storage in all study areas explored (although not uniformly so). This finding is of further interest as VME taxa are also often habitat formers/providers (correspondingly termed ecosystem engineers); hence, a co-benefit resulting from their presence (and protection) is the elevation of biodiversity levels and attendant functions (Buhl-Mortensen et al., 2010). In addition, as VME density-carbon relationships were similar to faunal density-carbon relationships, this may be potentially useful information for CCAMLR (or other regional management organisations) which exclusively (or particularly) monitor VME taxa. Such findings concerning VME taxa could be leveraged in marine spatial planning and protection prioritisation decisions in (and beyond) the study region.

4.5. A functional group approach for benthic assemblage analysis under environmental change

Several investigations, across both hemispheres, have employed a functional group approach to characterising benthic community structures and functions, for example, via grouping taxa by feeding mode (e.g., Jansen et al., 2020; Thyrring and Peck, 2021). A functional group approach has varied advantages, such as enabling the functionality of biodiversity to be examined and vastly reducing imagery appraisal times – the latter a renowned bottleneck between the acquisition of seabed images/video and desired outputs (Bowden et al., 2020), and ever more critical given the rate of environmental change, particularly, for example, in West Antarctica. Notably, in this study, different and multiple functional groups were major contributors to zoobenthic carbon storage across study areas (and sites). This finding indicates that, as at South Georgia (Barnes and Sands, 2017), all functional groups should be considered in view of protecting the carbon storage function of the benthos and benthic habitats. When comparing which groups majorly contributed at sites, MC1 and MC3 were the most similar – of all the sites, these sites were the closest in distance (<1 km) and situated within a relatively enclosed fjord basin.

4.6. Biological patterns and their environmental context, including sea-ice incidence

Consideration of the environment in which organisms live and habitats persist provides the opportunity to detect bio-environmental relationships (e.g., Cummings et al., 2018; Gutt et al., 2019) – helpful for understanding and predicting the effects of environmental change. In the current study, environmental data, of various spatial and temporal scales, were derived from in situ measurements, remote sensing and imagery, providing a contemporary environmental context to biological observations in the Scotia Arc study region. However, some of the environmental variables considered, and found to be coincident with zoobenthic carbon storage, are expected to be modified by climate change (Rogers et al., 2020), for example, long-projected sea-ice decline (Fox-Kemper et al., 2021). In the polar seas, sea-ice cover, including concentration, extent, timing and duration (the latter two features also referred to as "seasonality"), is regarded as a key environmental influencer of seabed habitat biodiversity and functionality (Lohrer et al., 2013; Clark et al., 2017; Pineda-Metz et al., 2020). Nonetheless, sea-ice cover (as well as other types of ice cover, e.g., ice shelf; Gilbert and Kittel, 2021) will likely be reduced due to the impacts of climate change

(depending on timescale, and societal action to mitigate [Pörtner et al., 2023]), with implications for marine community structuring and associated ecosystem services (Rogers et al., 2020; Cavanagh et al., 2021). Given the current climatic situation, it is particularly notable when environmental variables likely to modify with climate change are identified as potential drivers of contemporary biological patterns.

Greater zoobenthic carbon storage might be expected in areas void of extensive sea-ice cover, given potentially greater access by benthic fauna to primary-production-derived food, hence, for example, higher faunal densities (Smith et al., 2006; Lohrer et al., 2013). In this study, however, the opposite was observed (for both carbon storage and faunal density). Furthermore, when comparing southern (this study) and northern (Arctic; Souster et al., 2020) high-latitude study regions, C_{zoo} significantly differed between sea-ice-covered and non-sea-ice-covered sites (Fig. 6). For both of the polar regions, sites that experience sea-ice cover exhibited higher C_{zoo} values on average than sites that do not; however, for both sea-ice-cover conditions, the Antarctic study region had greater zoobenthic carbon storage means than the Arctic (though with large standard deviations). Again, this finding could be related to disparities in disturbance regime, where sites covered by sea ice are more shielded from disturbance than those that are not. This observation is similar to that of Frinault et al. (2022) at the Larsen C Ice Shelf front, in that biological variations (faunal densities) did not meet expectations based on ice-cover regime. The Antarctic observations are further interesting as the Bellingshausen Sea (where the sea-ice sites of the current study are situated) is considered a warm polar sea region, and the Weddell Sea (which hosts the Larsen C) is a cold polar sea region (of significance for bottom water formation; Meredith, 2013; Zhou et al., 2023). Thus, irrespective of being a warm or cold southern high-latitude marine region, similar unexpected density relationships appeared with sea-ice incidence. Whether the findings are related to sea ice in terms of sympagic primary production, and affiliated food-falls to the benthos, may also be important to determine (see Cautain et al., 2022).

4.7. Dropstones as potential islands of zoobenthic carbon storage

Dropstones are considered important physical seabed features, sometimes referred to as "islands", offering hard substrata/surfaces for benthic colonisation across swathes of soft/fine sediment (Ziegler et al., 2017), as well as providing platforms for elevation of suspension-feeding fauna into passing bottom currents in search of sustenance, as exemplified below the Filchner-Ronne Ice Shelf, southern Weddell Sea

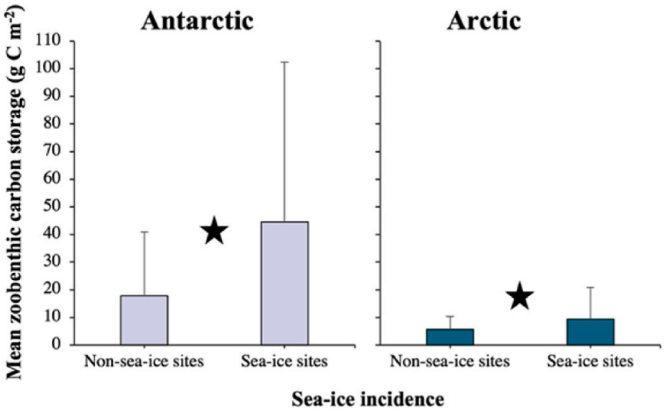

Fig. 6. Mean zoobenthic carbon storage (C_{zoo}; g C m^{-2}) of non-sea-ice and sea-ice sites for Antarctic and Arctic regions. Sea-ice sites correspond to those with a mean annual sea-ice cover of >10%. Data for the Antarctic are from this study, and for the Barents Sea (Arctic), from Souster et al. (2020). A black star indicates a statistically significant difference between non-sea-ice and sea-ice sites ($t = -3.480$ and -4.225 for the Antarctic and Arctic, respectively, with both p-values <0.001).

(Griffiths et al., 2021). In the present study, dropstones were relatively rare, constituting just a few percent of the seabed surface analysed, echoing findings of Post et al. (2020) for the Sabrina continental shelf, East Antarctica, where dropstones (in particular) accounted for <1% of the seafloor surface examined. Similar to results of Ziegler et al. (2017), for fjords of the western Antarctic Peninsula, the current study also found that dropstones generally supported higher morphotaxa richness and faunal densities and, in addition, zoobenthic carbon storage. Although in this study (as observed in others), dropstones were of low occurrence, given their association with ice-rafted debris, including of supraglacial provenance, it may be anticipated that dropstones will become more prevalent as icescapes transform in a warming world, especially in areas undergoing ice-shelf retreat and experiencing increased iceberg generation and transit. In consequence, respective areas may also eventually experience enhanced biodiversity (richness) and faunal densities, and, potentially, increased zoobenthic carbon storage, although other environmental factors (and changes to them) will also shape benthic community structure and function (Rogers et al., 2020).

4.8. Protection of benthic biodiversity aligns with safeguarding of zoobenthic carbon storage

Antarctica, its surrounding seas, and hence marine ecosystems and associated components, are currently under the protection of the Antarctic Treaty (due for renegotiation by 2048; Rogers et al., 2020) and attendant conventions, including those prohibiting mineral exploration (and exploitation), whaling and sealing, and restricting fishing activities, including pertaining to Antarctic krill, *Euphausia superba* – a key species of the Southern Ocean food web (Trathan and Hill, 2016; Rogers et al., 2020). Nonetheless, no convention presently exists directly addressing the safeguarding of Antarctic benthos (which includes most of Antarctica's known species), thus related functions. Nevertheless, as climate change intensifies and further ice-cover loss is experienced, the Southern Ocean and the Antarctic continental shelf will become more accessible; thus, novel challenges may be presented regarding the protection and endurance of benthic blue carbon estates of this southern high-latitude region. Further protections could be placed on blue carbon and possibly in a way that benefits international stakeholders – for example, via sharing the value of carbon stored by benthic or other marine habitats of the region between Antarctic Treaty nations, e.g., for incorporation into corresponding nationally determined contributions (as appropriate, and as per the 2015 Paris Agreement; UNFCCC, 2023). Given that benthic carbon storage and biodiversity have been shown to align, protecting blue carbon habitats and ecosystems could support both climate change mitigation and the safeguarding of biodiversity, and hence contribute to alleviating the associated crises.

5. Conclusions

Exploring four distinct continental shelf areas, all connected by the Scotia Arc, has provided an indication of how zoobenthic carbon storage capacity can vary along a southern polar gradient, with seabed habitats of the southernmost areas, i.e., those south of the ACC, currently supporting greater carbon storage (with a sixfold higher storage average presented). This exploration has also revealed that high-latitude zoobenthic carbon storage consistently aligned with faunal richness and density, as well as density of VME indicator taxa – the former finding supporting that the protection of benthic biodiversity could be complementary to the protection of benthic blue carbon (and vice versa), and the lattermost finding confirming that VME indicators can be important contributors to benthic blue carbon. Functional group contributions to carbon storage were also found to vary within and between study areas, advocating the notion of "collective protection" of high-latitude and polar benthic assemblages to best support their carbon storage function. In addition, and although other variables are likely

influential, zoobenthic blue carbon, in the confines of this study, appeared coincident with sea-ice cover – an environmental variable sensitive to ocean and atmospheric warming.

The current study has provided contemporary estimates of benthic blue carbon in terms of principally (epi-)zoobenthic carbon storage, as well as ecological and environmental baselines, and supports the protection of the benthos as a whole when considering, by example, the protection and endurance of their carbon storage function. Furthermore, findings may also contribute to evidence bases supporting high-latitude marine conservation measures and climate-considerate marine spatial planning.

CRediT authorship contribution statement

Bétina A.V. Frinault: Writing – review & editing, Writing – original draft, Visualization, Validation, Methodology, Investigation, Formal analysis, Data curation, Conceptualization. **David K.A. Barnes:** Writing – review & editing, Validation, Methodology, Investigation, Formal analysis, Data curation, Conceptualization.

Declaration of competing interest

The authors declare that they have no known competing financial interests or personal relationships that could have appeared to influence the work reported in this paper.

Data availability

The imagery analysed for this study can be found at the UK Polar Data Centre.

Acknowledgements

This paper was produced with funding from the UK Natural Environment Research Council grant NE/R011885/1 to B.A.V.F. and central funding to D.K.A.B. The authors would like to thank the officers and crew of the RRS *James Clark Ross*. The authors would also like to thank Laura Gerrish for cartography expertise, Kevin Arrigo and Gert van Dijken for kindly providing data concerning sea-ice concentration, primary production and sea surface temperature, Narissa Bax for providing carbon content values of southern Patagonian shelf zoobenthos and Alejandro Roman-Gonzalez for provision of the Marian Cove specimens. B.A.V.F. further extends thanks to Lisa Wedding and Chloë Strevens for review of the original manuscript. The authors would also like to thank the three anonymous reviewers for their comments leading to an improved manuscript.

Appendix A. Supplementary data

Supplementary data to this article can be found online at https://doi.org/10.1016/j.marenvres.2024.106621.

References

Alurralde, G., Fuentes, V.L., Maggioni, T., Movilla, J., Olariaga, A., Orejas, C., Schloss, I. R., Tatián, M., 2019. Role of suspension feeders in Antarctic pelagic-benthic coupling: trophic ecology and potential carbon sinks under climate change. Mar. Environ. Res. 152, 104790 https://doi.org/10.1016/j.marenvres.2019.104790.

Almond, P.M., Linse, K., Dreutter, S., Grant, S.M., Griffiths, H.J., Whittle, R.J., Mackenzie, M., Reid, W.D.K., 2021. In-situ image analysis of habitat heterogeneity and benthic biodiversity in the prince gustav channel, eastern antarctic Peninsula. Front. Mar. Sci. 8, 614496 https://doi.org/10.3389/fmars.2021.614496.

Anderson, M.J., Gorley, R.N., Clarke, K.R., 2008. PERMANOVA+ for PRIMER: Guide to Software and Statistical Methods. PRIMER-E, Plymouth, UK.

Arntz, W.E., Brey, T., Gallardo, V.A., 1994. Antarctic zoobenthos. Oceanogr. Mar. Biol. 32, 241–304.

Arrigo, K.R., van Dijken, G.L., Bushinsky, S., 2008. Primary production in the Southern Ocean, 1997–2006. J. Geophys. Res. Oceans 113, C08004. https://doi.org/10.1029/2007JC004551.

Arrigo, K.R., van Dijken, G.L., Strong, A.L., 2015. Environmental controls of marine productivity hot spots around Antarctica. J. Geophys. Res. Oceans 120, 5545–5565. https://doi.org/10.1002/2015JC010888.

Barnes, D.K.A., 2017. Polar zoobenthos blue carbon storage increases with sea ice losses, because across-shelf growth gains from longer algal blooms outweigh ice scour mortality in the shallows. Global Change Biol. 23, 5083–5091. https://doi.org/10.1111/gcb.13772.

Barnes, D.K.A., 2018. Blue carbon on polar and subpolar seabeds. In: Agarwal, R.K. (Ed.), Carbon Capture, Utilization and Sequestration. IntechOpen, London, UK, pp. 37–56. https://doi.org/10.5772/intechopen.78237.

Barnes, D.K.A., Bell, J.B., Bridges, A.E., Ireland, L., Howell, K.L., Martin, S.M., Sands, C. J., Mora Soto, A., Souster, T., Flint, G., Morley, S.A., 2021a. Climate Mitigation through Biological Conservation: Extensive and Valuable Blue Carbon Natural Capital in Tristan da Cunha's Giant Marine Protected Zone. Biology 10, 1339. https://doi.org/10.3390/biology10121339.

Barnes, D.K.A., Kuhn, G., Hillenbrand, C.D., Gromig, R., Koglin, N., Biskaborn, B.K., Frinault, B.A.V., Klages, J.P., Smith, E.C., Berger, S., Gutt, J., 2021b. Richness, growth, and persistence of life under an Antarctic ice shelf. Curr. Biol. 31, R1566–R1567. https://doi.org/10.1016/j.cub.2021.11.015.

Barnes, D.K.A., Sands, C.J., 2017. Functional group diversity is key to Southern Ocean benthic carbon pathways. PLoS One 12, e0179735. https://doi.org/10.1371/journal.pone.0179735.

Barnes, D.K.A., Sands, C.J., Cook, A., Howard, F., Roman-Gonzalez, A., Muñoz–Ramirez, C., Retallick, K., Scourse, J., Van Landeghem, K., Zwerschke, N., 2020. Blue carbon gains from glacial retreat along Antarctic fjords: what should we expect? Global Change Biol. 26, 2750–2755. https://doi.org/10.1111/gcb.15055.

Barnes, D.K.A., Sands, C.J., Richardson, A., Smith, N., 2019. Extremes in benthic ecosystem services; blue carbon natural capital shallower than 1000 m in isolated, small, and young ascension island's EEZ. Front. Mar. Sci. 6, 663. https://doi.org/10.3389/fmars.2019.00663.

Bax, N., Barnes, D.K.A., Pineda-Metz, S.E.A., Pearman, T., Diesing, M., Carter, S., Downey, R.V., Evans, C.D., Brickle, P., Baylis, A.M.M., Adler, A., Guest, A., Layton, K.K.S., Brewin, P.E., Bayley, D.T.I., 2022. Towards incorporation of blue carbon in Falkland Islands marine spatial planning: a multi-tiered approach. Front. Mar. Sci. 9, 872727 https://doi.org/10.3389/fmars.2022.872727.

Blair, T.C., McPherson, J.G., 1999. Grain-size and textural classification of coarse sedimentary particles. J. Sediment. Res. 69, 6–19. https://doi.org/10.2110/jsr.69.6.

Brasier, M.J., Barnes, D.K.A., Bax, N., Brandt, A., Christianson, A.B., Constable, A.J., Downey, R., Figuerola, B., Griffiths, H., Gutt, J., Lockhart, S., Morley, S.A., Post, A.L., Van de Putte, A., Saeedi, H., Stark, J.S., Sumner, M., Waller, C.L., 2021. Responses of Southern Ocean seafloor habitats and communities to global and local drivers of change. Front. Mar. Sci. 8, 622721 https://doi.org/10.3389/fmars.2021.622721.

Bray, J.R., Curtis, J.T., 1957. An ordination of the upland forest communities of southern Wisconsin. Ecol. Monogr. 27, 325–349. https://doi.org/10.2307/1942268.

Brooks, C.M., Chown, S.L., Douglass, L.L., Raymond, B.P., Shaw, J.D., Sylvester, Z.T., Torrens, C.L., 2020. Progress towards a representative network of Southern Ocean protected areas. PLoS One 15, e0231361. https://doi.org/10.1371/journal.pone.0231361.

Bowden, D.A., Rowden, A.A., Chin, C., Hempel, S., Wood, B., Hart, A., Clark, M.R., 2020. Best practice in seabed image analysis for determining taxa, habitat, or substrata distributions: New Zealand Aquatic Environment and Biodiversity Report No. 239. Fisheries New Zealand, Wellington, New Zealand 61. https://fs.fish.govt.nz/Doc/24797/AEBR-239-Best-Practice-In-Seabed-Image-Analysis.pdf.ashx.

Buhl-Mortensen, L., Vanreusel, A., Gooday, A.J., Levin, L.A., Priede, I.G., Buhl-Mortensen, P., Gheerardyn, H., King, N.J., Raes, M., 2010. Biological structures as a source of habitat heterogeneity and biodiversity on the deep ocean margins. Mar. Ecol. 31, 21–50. https://doi.org/10.1111/j.1439-0485.2010.00359.x.

Casado, M., Hébert, R., Faranda, D., Landais, A., 2023. The quandary of detecting the signature of climate change in Antarctica. Nat. Clim. Change 13, 1082–1088. https://doi.org/10.1038/s41558-023-01791-5.

Cartapanis, O., Bianchi, D., Jaccard, S., Galbraith, E.D., 2016. Global pulses of organic carbon burial in deep-sea sediments during glacial maxima. Nat. Commun. 7, 10796 https://doi.org/10.1038/ncomms10796.

Cavan, E.L., Hill, S.L., 2022. Commercial fishery disturbance of the global ocean biological carbon sink. Global Change Biol. 28, 1212–1221. https://doi.org/10.1111/gcb.16019.

Cavanagh, R.D., Melbourne-Thomas, J., Grant, S.M., Barnes, D.K.A., Hughes, K.A., Halfter, S., Meredith, M.P., Murphy, E.J., Trebilco, R., Hill, S.L., 2021. Future risk for Southern Ocean ecosystem services under climate change. Front. Mar. Sci. 7, 615214 https://doi.org/10.3389/fmars.2020.615214.

CCAMLR, 2009. VME Taxa Classification Guide. CCAMLR, Hobart, Tasmania, Australia, p. 4.

CCAMLR, 2019. CCAMLR VME Registry. CCAMLR, Hobart, Tasmania, Australia.

Cautain, I.J., Last, K.S., McKee, D., Bluhm, B.A., Renaud, P.E., Ziegler, A.F., Narayanaswamy, B.E., 2022. Uptake of sympagic organic carbon by the Barents Sea benthos linked to sea ice seasonality. Front. Mar. Sci. 9, 1009303 https://doi.org/10.3389/fmars.2022.1009303.

Clark, G.F., Stark, J.S., Palmer, A.S., Riddle, M.J., Johnston, E.L., 2017. The roles of Sea-Ice, light and sedimentation in structuring shallow antarctic benthic communities. PLoS One 12, e0168391. https://doi.org/10.1371/journal.pone.0168391.

Clarke, A., Aronson, R.B., Crame, J.A., Gili, J.-M., Blake, D.B., 2004. Evolution and diversity of the benthic fauna of the Southern Ocean continental shelf. Antarct. Sci. 16, 559–568. https://doi.org/10.1017/S0954102004002329.

Clarke, K.R., 1993. Nonparametric multivariate analyses of changes in community structure. Aust. J. Ecol. 18, 117–143. https://doi.org/10.1111/j.1442-9993.1993.tb00438.x.

Clarke, K.R., Ainsworth, M.A., 1993. Method of linking multivariate community structure to environmental variables. Mar. Ecol. Prog. Ser. 92, 205–219. https://doi.org/10.3354/meps092205.
Clarke, K.R., Gorley, R.N., 2015. PRIMER V7: User Manual/Tutorial. PRIMER-E, Plymouth, UK.
Clarke, K.R., Gorley, R.N., Somerfield, P.J., Warwick, R.M., 2014. Change in Marine Communities: an Approach to Statistical Analysis and Interpretation, third ed. PRIMER-E, Plymouth, UK, p. 262.
Clarke, K.R., Green, R.H., 1988. Statistical design and analysis for a 'biological effects' study. Mar. Ecol. Prog. Ser. 46, 213–226. https://doi.org/10.3354/meps046213.
Clarke, A., Johnston, N.M., 2003. Antarctic marine benthic diversity. Oceanogr. Mar. Biol. 41, 47–114. https://doi.org/10.1201/9780203180570.
Clarke, K.R., Somerfield, P.J., Gorley, R.N., 2008. Testing of null hypotheses in exploratory community analyses: similarity profiles and biota-environment linkage. J. Exp. Mar. Biol. Ecol. 366, 56–69. https://doi.org/10.1016/j.jembe.2008.07.009.
Cummings, V.J., Bowden, D.A., Pinkerton, M.H., Halliday, N.J., Hewitt, J.E., 2021. Ross Sea benthic ecosystems: macro- and mega-faunal community patterns from a multi-environment Survey. Front. Mar. Sci. 8, 629787 https://doi.org/10.3389/fmars.2021.629787.
Cummings, V.J., Hewitt, J.E., Thrush, S.F., Marriott, P.M., Halliday, N.J., Norkko, A., 2018. Linking Ross sea coastal benthic communities to environmental conditions: documenting baselines in a spatially variable and changing world. Front. Mar. Sci. 5, 232. https://doi.org/10.3389/fmars.2018.00232.
Dayton, P., Jarrell, S., Kim, S., Thrush, S., Hammerstrom, K., Slattery, M., Parnell, E., 2016. Surprising episodic recruitment and growth of Antarctic sponges: implications for ecological resilience. J. Exp. Mar. Biol. Ecol. 482, 38–55. https://doi.org/10.1016/j.jembe.2016.05.001.
Dayton, P.K., Kim, S., Jarrell, S.C., Oliver, J.S., Hammerstrom, K., Fisher, J.L., O'Connor, K., Barber, J.S., Robilliard, G., Barry, J., Thurber, A.R., Conlan, K., 2013. Recruitment, growth and mortality of an antarctic Hexactinellid sponge, *Anoxycalyx joubini*. PLoS One 8, e56939. https://doi.org/10.1371/journal.pone.0056939.
Deppeler, S.L., Davidson, A.T., 2017. Southern Ocean phytoplankton in a changing climate. Front. Mar. Sci. 4, 40. https://doi.org/10.3389/fmars.2017.00040.
De Broyer, C., Koubbi, P., Griffiths, H., Raymond, B., d'Udekem d'Acoz, C., Van de Putte, A., Danis, B., David, B., Grant, S., Gutt, J., Held, C., Hosie, G., Huettmann, F., Post, A., Ropert-Coudert, Y., 2014. Biogeographic Atlas of the Southern Ocean. Scientific Committee on Antarctic Research, Cambridge, UK, p. 510.
DESNZ, 2023. 2022 UK Greenhouse Gas Emissions, Provisional Figures. DESNZ, London, UK. https://assets.publishing.service.gov.uk/media/6424b8b83d885d000fdade9b/2022_Provisional_emissions_statistics_report.pdf.
Domack, E., Ishman, S., Leventer, A., Sylva, S., Willmott, V., Huber, B., 2005. A chemotrophic ecosystem found beneath Antarctic Ice Shelf. Eos 86, 269–272. https://doi.org/10.1029/2005eo290001.
Dorschel, B., Hehemann, L., Viquerat, S., Warnke, F., Dreutter, S., Schulze Tenberge, Y., Accettella, D., An, L., Barrios, F., Bazhenova, E.A., Black, J., Bohoyo, F., Davey, Craig, de Santis, L., Escutia Dotti, C., Fremand, A.C., Fretwell, P.T., Gales, J. A., Gao, J., Gasperini, L., Greenbaum, J.S., Henderson Jencks, J., Hogan, K.A., Hong, J.K., Jakobsson, M., Jensen, L., Kool, J., Larin, S., Larter, R.D., Leitchenkov, G. L., Loubrieu, B., Mackay, K., Mayer, L., Millan, R., Morlighem, M., Navidad, F., Nitsche, F.-O., Nogi, Y., Pertuisot, C., Post, A.L., Pritchard, H.D., Purser, A., Rebesco, M., Rignot, E., Roberts, J.L., Rovere, M., Ryzhov, I., Sauli, C., Schmitt, T., Silvano, A., Smith, J.E., Snaith, H., Tate, A.J., Tinto, K., Vandenbossche, P., Weatherall, P., Wintersteller, P., Yang, C., Zhang, T., Arndt, J.E., 2022. The international bathymetric Chart of the Southern Ocean version 2. Sci. Data 9, 275. https://doi.org/10.1038/s41597-022-01366-7.
Dowdeswell, J.A., Bamber, J.L., 2007. Keel depths of modern Antarctic icebergs and implications for sea-floor scouring in the geological record. Mar. Geol. 243, 120–131. https://doi.org/10.1016/j.margeo.2007.04.008.
Everitt, B., 1980. Cluster analysis. Qual. Quantity 14, 75–100. https://doi.org/10.1007/BF00154794.
FAO, 2009. International Guidelines for the Management of Deep-Sea Fisheries in the High Seas. FAO, Rome, Italy, p. 73.
Fillinger, L., Janussen, D., Lundalv, T., Richter, C., 2013. Rapid glass sponge expansion after climate-induced Antarctic ice shelf collapse. Curr. Biol. 23, 1330–1334. https://doi.org/10.1016/j.cub.2013.05.051.
Fox-Kemper, B., Hewitt, H.T., Xiao, C., Aðalgeirsdóttir, G., Drijfhout, S.S., Edwards, T.L., Golledge, N.R., Hemer, M., Kopp, R.E., Krinner, G., Mix, A., Notz, D., Nowicki, S., Nurhati, I.S., Ruiz, L., Sallée, J.-B., Slangen, A.B.A., Yu, Y., 2021. Ocean, cryosphere and sea level change. In: Masson-Delmotte, V., Zhai, P., Pirani, A., Connors, S.L., Péan, C., Berger, S., Caud, N., Chen, Y., Goldfarb, L., Gomis, M.I., Huang, M., Leitzell, K., Lonnoy, E., Matthews, J.B.R., Maycock, T.K., Waterfield, T., Yelekçi, O., Yu, R., Zhou, B. (Eds.), Climate Change 2021: the Physical Science Basis. Contribution of Working Group I to the Sixth Assessment Report of the Intergovernmental Panel on Climate Change. Cambridge University Press, Cambridge, United Kingdom, pp. 1211–1362. https://doi.org/10.1017/9781009157896.011.
Friedlingstein, P., O'Sullivan, M., Jones, M.W., Andrew, R.M., Bakker, D.C.E., Hauck, J., Landschützer, P., Le Quéré, C., Luijkx, I.T., Peters, G.P., Peters, W., Pongratz, J., Schwingshackl, C., Sitch, S., Canadell, J.G., Ciais, P., Jackson, R.B., Alin, S.R., Anthoni, P., Barbero, L., Bates, N.R., Becker, M., Bellouin, N., Decharme, B., Bopp, L., Brasika, I.B.M., Cadule, P., Chamberlain, M.A., Chandra, N., Chau, T.-T.-T., Chevallier, F., Chini, L.P., Cronin, M., Dou, X., Enyo, K., Evans, W., Falk, S., Feely, R. A., Feng, L., Ford, D.J., Gasser, T., Ghattas, J., Gkritzalis, T., Grassi, G., Gregor, L., Gruber, N., Gürses, Ö., Harris, I., Hefner, M., Heinke, J., Houghton, R.A., Hurtt, G.C., Iida, Y., Ilyina, T., Jacobson, A.R., Jain, A., Jarníková, T., Jersild, A., Jiang, F., Jin, Z., Joos, F., Kato, E., Keeling, R.F., Kennedy, D., Klein Goldewijk, K., Knauer, J., Korsbakken, J.I., Körtzinger, A., Lan, X., Lefèvre, N., Li, H., Liu, J., Liu, Z., Ma, L., Marland, G., Mayot, N., McGuire, P.C., McKinley, G.A., Meyer, G., Morgan, E.J., Munro, D.R., Nakaoka, S.-I., Niwa, Y., O'Brien, K.M., Olsen, A., Omar, A.M., Ono, T., Paulsen, M., Pierrot, D., Pocock, K., Poulter, B., Powis, C.M., Rehder, G., Resplandy, L., Robertson, E., Rödenbeck, C., Rosan, T.M., Schwinger, J., Séférian, R., Smallman, T.L., Smith, S.M., Sospedra-Alfonso, R., Sun, Q., Sutton, A.J., Sweeney, C., Takao, S., Tans, P.P., Tian, H., Tilbrook, B., Tsujino, H., Tubiello, F., van der Werf, G. R., van Ooijen, E., Wanninkhof, R., Watanabe, M., Wimart-Rousseau, C., Yang, D., Yang, X., Yuan, W., Yue, X., Zaehle, S., Zeng, J., Zheng, B., 2023. Global carbon budget 2023. Earth Syst. Sci. Data 15, 5301–5369. https://doi.org/10.5194/essd-15-5301-2023.
Frinault, B.A.V., Christie, F.D.W., Fawcett, S.E., Flynn, R.F., Hutchinson, K.A., Montes Strevens, C.M.J., Taylor, M.L., Woodall, L.C., Barnes, D.K.A., 2022. Antarctic seabed assemblages in an ice-shelf-adjacent polynya, western Weddell Sea. Biology 11, 1705. https://doi.org/10.3390/biology11121705.
Frinault, B.A.V., Barnes, D.K.A., Biskaborn, B.K., Gromig, R., Hillenbrand, C.-D., Klages, J.P., Koglin, N., Kuhn, G., 2023. Spatial competition in a global disturbance minimum; the seabed under an antarctic ice shelf. Sci. Total Environ. 903, 166157 https://doi.org/10.1016/j.scitotenv.2023.166157.
Gilbert, E., Kittel, C., 2021. Surface melt and runoff on Antarctic ice shelves at 1.5°C, 2°C, and 4°C of future warming. Geophys. Res. Lett. 48, e2020GL091733 https://doi.org/10.1029/2020GL091733.
Gogarty, B., McGee, J., Barnes, D.K.A., Sands, C.J., Bax, N., Haward, M., Downey, R., Moreau, C., Moreno, B., Held, C., Paulsen, M.L., 2020. Protecting Antarctic blue carbon: as marine ice retreats can the law fill the gap? Clim. Pol. 20, 149–162. https://doi.org/10.1080/14693062.2019.1694482.
Grant, S.M., Hill, S.L., Trathan, P.N., Murphy, E.J., 2013. Ecosystem services of the Southern Ocean: trade-offs in decision-making. Antarct. Sci. 25, 603–617. https://doi.org/10.1017/S0954102013000308.
Griffiths, H.J., Anker, P., Linse, K., Maxwell, J., Post, A., Stevens, C., Tulaczyk, S., Smith, J.A., 2021. Breaking all the rules: the first recorded hard substrate sessile benthic community far beneath an Antarctic ice shelf. Front. Mar. Sci. 8, 642040 https://doi.org/10.3389/fmars.2021.642040.
Greiner, J.T., McGlathery, K.J., Gunnell, J., McKee, B.A., 2013. Seagrass restoration enhances "blue carbon" sequestration in coastal waters. PLoS One 8, e72469. https://doi.org/10.1371/journal.pone.0072469.
Gros, C., Jansen, J., Untiedt, C., Pearman, T.R.R., Downey, R., Barnes, D.K.A., Bowden, D.A., Welsford, D.C., Hill, N.A., 2023. Identifying vulnerable marine ecosystems: an image-based vulnerability index for the Southern Ocean seafloor. ICES J. Mar. Sci. 80, 972–986. https://doi.org/10.1093/icesjms/fsad021.
Gutt, J., Arndt, J., Kraan, C., Dorschel, B., Schröder, M., Bracher, A., Piepenburg, D., 2019. Benthic communities and their drivers: a spatial analysis off the Antarctic Peninsula. Limnol. Oceanogr. 64, 2341–2357. https://doi.org/10.1002/lno.11187.
Gutt, J., Isla, E., Xavier, J.C., Adams, B.J., Ahn, I.Y., Cheng, C.C., Colesie, C., Cummings, V.J., Di Prisco, G., Griffiths, H., Hawes, I., Hogg, I., Mcintyre, T., Meiners, K.M., Pearce, D.A., Peck, L., Piepenburg, D., Reisinger, R.R., Saba, G.K., Schloss, I.R., Signori, C.N., Smith, C.R., Vacchi, M., Verde, C., Wall, D.H., 2021. Antarctic ecosystems in transition – life between stresses and opportunities. Biol. Rev. Camb. Phil. Soc. 96, 798–821. https://doi.org/10.1111/brv.12679.
Henley, S.F., Cavan, E.L., Fawcett, S.E., Kerr, R., Monteiro, T., Sherrell, R.M., Bowie, A. R., Boyd, P.W., Barnes, D.K.A., Schloss, I.R., Marshall, T., Flynn, R., Smith, S., 2020. Changing biogeochemistry of the southern Ocean and its ecosystem implications. Front. Mar. Sci. 7, 581. https://doi.org/10.3389/fmars.2020.00581.
Holloway, S., Burnard, K., 2009. Storage capacity and containment issues for carbon dioxide capture and geological storage on the UK continental shelf. Proc. Inst. Mech. Eng.: J. Power Energy 223, 239–248. https://doi.org/10.1243/09576509JPE650.
Howard, J., Hoyt, S., Isensee, K., Pidgeon, E., Telszewski, M. (Eds.), 2014. Coastal Blue Carbon: Methods for Assessing Carbon Stocks and Emissions Factors in Mangroves, Tidal Salt Marshes, and Seagrass Meadows. Conservation International, Intergovernmental Oceanographic Commission of UNESCO, International Union for Conservation of Nature, Arlington, VA, USA, p. 182.
Huang, B., Liu, C., Banzon, V., Freeman, E., Graham, G., Hankins, B., Smith, T., Zhang, H.-M., 2020. Improvements of the daily Optimum interpolation Sea Surface temperature (DOISST) version 2.1. J. Clim. 34, 2923–2939. https://doi.org/10.1175/JCLI-D-20-0166.1.
IPCC, 2022. Summary for policymakers. In: Pörtner, H.-O., Roberts, D.C., Tignor, M., Poloczanska, E.S., Mintenbeck, K., Alegría, A., Craig, M., Langsdorf, S., Löschke, S., Möller, V., Okem, A., Rama, B. (Eds.), Climate Change 2022: Impacts, Adaptation and Vulnerability. Contribution of Working Group II to the Sixth Assessment Report of the Intergovernmental Panel on Climate Change. Cambridge University Press, Cambridge, UK and New York, NY, USA, pp. 3–33. https://doi.org/10.1017/9781009325844.001.
IPCC, 2023. Summary for policymakers. In: Lee, H., Romero, J. (Eds.), Climate Change 2023: Synthesis Report. Contribution of Working Groups I, II and III to the Sixth Assessment Report of the Intergovernmental Panel on Climate Change [Core Writing Team. IPCC, Geneva, Switzerland, pp. 1–34. https://doi.org/10.59327/IPCC/AR6-9789291691647.001.
Isla, E., Gerdes, D., Palanques, A., Teixidó, N., Arntz, W., Puig, P., 2006. Relationships between Antarctic coastal and deep-sea particle fluxes: implications for the deep-sea benthos. Polar Biol. 29, 249–256. https://doi.org/10.1007/s00300-005-0046-9.
Jansen, J., Dunstan, P.K., Hill, N.A., Koubbi, P., Melbourne-Thomas, J., Causse, R., Johnson, C.R., 2020. Integrated assessment of the spatial distribution and structural dynamics of deep benthic marine communities. Ecol. Appl. 30, 02065 https://doi.org/10.1002/eap.2065.

Langenkämper, D., Zurowietz, M., Schoening, T., Nattkemper, T.W., 2017. Biigle 2.0 - browsing and annotating large marine image collections. Front. Mar. Sci. 4, 83. https://doi.org/10.3389/fmars.2017.00083.

Lockhart, S.J., Hocevar, J., 2021. Combined abundance of all vulnerable marine ecosystem indicator taxa inadequate as sole determiner of vulnerability, antarctic Peninsula. Front. Mar. Sci. 8, 577761. https://10.3389/fmars.2021.577761.

Lohrer, A.M., Cummings, V.J., Thrush, S.F., 2013. Altered Sea ice thickness and permanence affects benthic ecosystem functioning in coastal Antarctica. Ecosystems 16, 224–236. https://doi.org/10.1007/s10021-012-9610-7.

Luo, J., Xie, Y., Hou, M.Z., Xiong, Y., Wu, X., Truitt Lüddeke, C., Huang, L., 2023. Advances in subsea carbon dioxide utilization and storage. Energy Rev. 2, 100016 https://doi.org/10.1016/j.enrev.2023.100016.

Mcleod, E., Chmura, G.L., Bouillon, S., Salm, R.V., Björk, M., Duarte, C.M., Lovelock, C. E., Schlesinger, W.H., Silliman, B.R., 2011. A blueprint for blue carbon: toward an improved understanding of the role of vegetated coastal habitats in sequestering CO_2. Front. Ecol. Environ. 9, 552–560. https://doi.org/10.1890/110004.

Meier, W.N., Fetterer, F., Windnagel, A.K., Stewart, J.S., 2021. NOAA/NSIDC Climate Data Record of Passive Microwave Sea Ice Concentration. National Snow and Ice Data Center, Boulder CO, USA. https://doi.org/10.7265/efmz-2t65.

Meredith, M.P., 2013. Replenishing the abyss. Nat. Geosci. 6, 166. https://doi.org/10.1038/ngeo1743.

Mildrexler, D.J., Berner, L.T., Law, B.E., Birdsey, R.A., Moomaw, W.R., 2020. Large trees dominate carbon storage in forests east of the cascade crest in the United States Pacific Northwest. Front. For. Glob. Change 3, 594274. https://doi.org/10.3389/ffgc.2020.594274.

Miller, R.J., Hocevar, J., Stone, R.P., Fedorov, D.V., 2012. Structure-forming corals and sponges and their use as fish habitat in Bering Sea submarine canyons. PLoS One 7, e33885. https://doi.org/10.1371/journal.pone.0033885.

Morley, S.A., Souster, T.A., Vause, B.J., Gerrish, L., Peck, L.S., Barnes, D.K.A., 2022. Benthic biodiversity, carbon storage and the potential for increasing negative feedbacks on climate change in shallow waters of the antarctic Peninsula. Biology 11, 320. https://doi.org/10.3390/biology11020320.

Niemann, H., Fischer, D., Graffe, D., Knittel, K., Montiel, A., Heilmayer, O., Nöthen, K., Pape, T., Kasten, S., Bohrmann, G., Boetius, A., Gutt, J., 2009. Biogeochemistry of a low-activity cold seep in the Larsen B area, western Weddell Sea, Antarctica. Biogeosciences 6, 2383–2395. https://doi.org/10.5194/bg-6-2383-2009.

Peck, L.S., Barnes, D.K.A., Cook, A.J., Fleming, A.H., Clarke, A., 2010. Negative feedback in the cold: ice retreat produces new carbon sinks in Antarctica. Global Change Biol. 16, 2614–2623. https://doi.org/10.1111/j.1365-2486.2009.02071.x.

Pineda-Metz, S.E.A., Gerdes, D., 2018. Seabed images versus corer sampling: a comparison of two quantitative approaches for the analysis of marine benthic communities in the southern Weddell Sea (Southern Ocean). Polar Biol. 41, 515–526. https://doi.org/10.1007/s00300-017-2211-3.

Pineda-Metz, S.E.A., Gerdes, D., Richter, C., 2020. Benthic fauna declined on a whitening Antarctic continental shelf. Nat. Commun. 11, 2226. https://doi.org/10.1038/s41467-020-16093-z.

Pörtner, H.-O., Scholes, R.J., Arneth, A., Barnes, D.K.A., Burrows, M.T., Diamond, S.E., Duarte, C.M., Kiessling, W., Leadley, P., Managi, S., McElwee, P., Midgley, G., Ngo, H.T., Obura, D., Pascual, U., Sankaran, M., Shin, Y.J., Val, A.L., 2023. Overcoming the coupled climate and biodiversity crises and their societal impacts. Science 380, eabl4881. https://doi.org/10.1126/science.abl4881.

Post, A.L., Lavoie, C., Domack, E.W., Leventer, A., Fernandez, R., Shipboard Scientific Party, 2020. Dropstones on a glaciated continental shelf as key habitat, Sabrina Shelf, East Antarctica. In: Harris, P.T., Baker, E. (Eds.), Seafloor Geomorphology as Benthic Habitat: GeoHab Atlas of Seafloor Geomorphic Features and Benthic Habitats, second ed. Elsevier, Amsterdam, The Netherlands; Oxford, UK; and Cambridge, MA, USA, pp. 641–653. https://doi.org/10.1016/B978-0-12-814960-7.00038-5.

Post, A.L., Lavoie, C., Domack, E.W., Leventer, A., Shevenell, A., Fraser, A.D., 2017. Environmental drivers of benthic communities and habitat heterogeneity on an East Antarctic shelf. Antarct. Sci. 29, 17–32. https://doi.org/10.1017/S0954102016000468.

Rogers, A.D., Frinault, B.A.V., Barnes, D.K.A., Bindoff, N.L., Downie, R., Ducklow, H.W., Friedlander, A.S., Hart, T., Hill, S.L., Hofmann, E.E., Linse, K., McMahon, C.R., Murphy, E.J., Pakhomov, E.A., Reygondeau, G., Staniland, I.J., Wolf-Gladrow, D.A., Wright, R.M., 2020. Antarctic futures: an assessment of climate-driven changes on ecosystem structure, function and service provision in the Southern Ocean. Ann. Rev. Mar. Sci 12, 87–120. https://doi.org/10.1146/annurev-marine-010419-011028.

Sands, C.J., Zwerschke, N., Bax, N., Barnes, D.K.A., Moreau, C., Downey, R., Moreno, B., Held, C., Paulsen, M., 2023. Perspective: the growing potential of Antarctic blue carbon. In: Kappel, E.S., Cullen, V., Costello, M.J., Galgani, L., Gordó-Vilaseca, C., Govindarajan, A., Kouhi, S., Lavin, C., McCartin, L., Müler, J.D., Pirenne, B., Tanhua, T., Zhao, Q., Zhao, S. (Eds.), Frontiers in Ocean Observing: Emerging Technologies for Understanding and Managing a Changing Ocean, 36. Oceanography, pp. 16–17. https://doi.org/10.5670/oceanog.2023.s1.5. Supplement 1.

Siegert, M.J., Bentley, M.J., Atkinson, A., Bracegirdle, T.J., Convey, P., Davies, B., Downie, R., Hogg, A.E., Holmes, C., Hughes, K.A., Meredith, M.P., Ross, N., Rumble, J., Wilkinson, J., 2023. Antarctic extreme events. Front. Environ. Sci. 11, 1229283 https://doi.org/10.3389/fenvs.2023.1229283.

Smale, D.A., Barnes, D.K.A., Fraser, K.P.P., Peck, L.S., 2008. Benthic community response to iceberg scouring at an intensely disturbed shallow water site at Adelaide Island, Antarctica. Mar. Ecol. Prog. Ser. 355, 85–94. https://doi.org/10.3354/meps07311.

Smith, C.R., Mincks, S., DeMaster, D.J., 2006. A synthesis of bentho-pelagic coupling on the Antarctic shelf: food banks, ecosystem inertia and global climate change. Deep Sea Res. II 53, 875–894. https://doi.org/10.1016/j.dsr2.2006.02.001.

Song, S., Ding, Y., Li, W., Meng, Y., Zhou, J., Gou, R., Zhang, C., Ye, S., Saintilan, N., Krauss, K.W., Crooks, S., Lv, S., Lin, G., 2023. Mangrove reforestation provides greater blue carbon benefit than afforestation for mitigating global climate change. Nat. Commun. 14, 756. https://doi.org/10.1038/s41467-023-36477-1.

Souster, T.A., Barnes, D.K.A., Hopkins, J., 2020. Variation in zoobenthic blue carbon in the Arctic's Barents Sea shelf sediments. Philos. Trans. R. Soc. A 378, 20190362. https://doi.org/10.1098/rsta.2019.0362.

Souster, T.A., Barnes, D.K.A., Primicerio, R., Jørgensen, L.L., 2024. Quantifying zoobenthic blue carbon storage across habitats within the Arctic's Barents Sea. Front. Mar. Sci. 10, 1260884 https://doi.org/10.3389/fmars.2023.1260884.

Steffen, W., Grinevald, J., Crutzen, P., McNeill, J., 2011. The Anthropocene: conceptual and historical perspectives. Philos. Trans. R. Soc. A 369, 842–867. https://doi.org/10.1098/rsta.2010.0327.

Teixidó, N., Garrabou, J., Gutt, J., Arntz, W.E., 2007. Iceberg disturbance and successional spatial patterns: the case of the shelf antarctic benthic communities. Ecosystems 10, 143–158. https://doi.org/10.1007/s10021-006-9012-9.

Thyrring, J., Peck, L.S., 2021. Global gradients in intertidal species richness and functional groups. Elife 10, e64541. https://doi.org/10.7554/eLife.64541.

Trathan, P.N., Hill, S.L., 2016. The importance of krill predation in the Southern Ocean. In: Siegel, V. (Ed.), Biology and Ecology of Antarctic Krill. Springer, Cham, Switzerland, pp. 321–350. https://doi.org/10.1007/978-3-319-29279-3_9.

UNFCCC, 2023. Nationally determined contributions under the Paris Agreement. Synthesis report by the secretariat. https://unfccc.int/sites/default/files/resource/cma2023_12.pdf.

Vilas, D., Coll, M., Pedersen, T., Corrales, X., Filbee-Dexter, K., Pedersen, M.F., Norderhaug, K.M., Fredriksen, S., Wernberg, T., Ramírez-Llodra, E., 2020. Kelp-carbon uptake by Arctic deep-sea food webs plays a noticeable role in maintaining ecosystem structural and functional traits. J. Mar. Syst. 203, 103268 https://doi.org/10.1016/j.jmarsys.2019.103268.

Zhou, S., Meijers, A.J.S., Meredith, M.P., Povl Abrahamsen, E., Holland, P.R., Silvano, A., Sallée, J.-B., Østerhus, S., 2023. Slowdown of Antarctic Bottom Water export driven by climatic wind and sea-ice changes. Nat. Clim. Change 13, 701–709. https://doi.org/10.1038/s41558-023-01695-4.

Ziegler, A.F., Smith, C.R., Edwards, K.F., Vernet, M., 2017. Glacial dropstones: islands enhancing seafloor species richness of benthic megafauna in West Antarctic Peninsula fjords. Mar. Ecol. Prog. Ser. 583, 1–14. https://doi.org/10.3354/meps12363.

Zwerschke, N., Sands, C.J., Roman-Gonzalez, A., Barnes, D.K.A., Guzzi, A., Jenkins, S., Muñoz-Ramírez, C., Scourse, J., 2022. Quantification of blue carbon pathways contributing to negative feedback on climate change following glacier retreat in West Antarctic fjords. Global Change Biol. 28, 8–20. https://doi.org/10.1111/gcb.15898.